POLITECNICO DI TORINO

Corso di Laurea in Ingegneria Biomedica

Tesi di Laurea Magistrale

Novel composite biomaterials based on polyurethane injectable hydrogels and ordered mesoporous nanoparticles for effective and non-invasive drug delivery

Relatore
prof. Gianluca Ciardelli

Correlatore:
dr. Georgia Charalambopoulou

Candidata
Claudia Agus

MARZO 2018

Ai miei genitori

ABSTRACT

Drug delivery is a method or a process of administering a pharmaceutical compound to achieve a therapeutic effect in humans or animals.[1]

Conventional administration of drugs is characterized by limited effectiveness, poor biodistribution, and lack of selectivity.[2] Standard routes of drug administration, such as oral and intravenous, are not characterized by a 100% efficiency, because the substance spreads inside the body and not only in the target site, i.e. the disease area where the drug should be heading. This also causes side effects, which usually are light and tolerable, but can be very dangerous in case of serious diseases, like cancer, that requires strong drugs. Hence, the idea to create new, advanced drug delivery systems that can encapsulate drugs and carry them directly to the chosen site, can increase the efficiency and allow to reduce the dose and limit the side effects.

The use of nanoparticles is becoming more and more important for the search of such novel therapeutic platforms, since they allow to keep the drug encapsulated until they reach the target site, protecting it from hostile environments (e.g. acid stomach environment) but also protecting the body from side effects.

The main aim of this master thesis, which was realized through the collaboration of Politecnico di Torino (Dipartimento di Ingegneria Meccanica e Aerospaziale) and the INRASTES/INN Institutes of the National Center for Scientific Research "Demokritos" (Athens, Greece), has been to develop a composite drug delivery system that could be suitable for non-invasive therapies such as the treatment of non-healing chronic skin wounds. The idea is to combine two different types of materials to make an effective platform for delivering therapeutic compounds: a thermosensitive hydrogel and ordered mesoporous nanoparticles. In this way, it is possible to exploit the significant advantages of these two families of materials and blend them to achieve the therapeutic goal in the most efficient way.

Hydrogels are polymeric materials, which are capable of retaining large amounts of water in their three-dimensional hydrophilic polymer networks. They are characterized by a soft and rubbery consistency, enabling them to mimic specific aspects of tissues microenvironment.[3,4] The use of hydrogels for in vivo applications is considered to be advantageous due to their high biocompatibility, which is promoted by the large amounts of water that they can incorporate and their physicochemical similarity to the native extracellular matrix, both compositionally (particularly in the case of carbohydrate-based hydrogels) and mechanically. In this work, the amphiphilic poly(etherurethane) CHP407 has been used, whose synthesis has been reported very recently by Boffito and coworkers.[3] CHP407 is obtained from poloxamer P407, a Food and Drug Administration approved PEO-PPO-PEO triblock copolymer, which imparts to the gel superior strength, lower critical gelation concentration and lower critical gelation temperature behavior, faster gelation kinetics, as well as higher stability in physiological conditions. Indeed, the solution of this polymer in water-based media can form a biocompatible injectable thermosensitive

hydrogel with a lower critical gelation temperature (LCGT) behavior, which means that it forms a gel by heating it above a certain temperature and remains stable in a gel form in a certain interval of temperatures above the LCGT. Indeed, it is thermosensitive because the sol-gel transition is driven exclusively by temperature: in this case, under 37 °C the polymer is in the liquid phase, which makes it even more interesting as this corresponds to the human body temperature.

On the other hand, the use of ordered mesoporous materials (OMMs) also offers significant advantages. According to the IUPAC definition, mesoporous materials are those having pores with diameter in the range of 2–50nm. OMMs were chosen due to their particular features, which make them very good candidate materials for the encapsulation of active compounds. Indeed OMMs have a very high specific surface area and pore volume that allows to incorporate a large amount of a specific drug. Besides, a tailorable pore size makes them suitable for the encapsulation of different molecules with various sizes. Furthermore they can guarantee a stable payload as it is protected by the inert porous matrix and thus it does not disintegrate easily before it gets released to the target site.

These two families of materials, i.e. hydrogels and ordered mesoporous nanoparticles, were combined with each other using different concentrations of hydrogel-15%w/V and 20%w/V-, different amounts of particles and various protocols for blending them. A significant effort was devoted to optimise as much as possible the obtained composite systems aiming to maximize the content of the dispersed OMS and OMC nanoparticles, which were successfully encapsulated within the hydrogels (without affecting their structure and gelation behaviour) up to a final concentration of 20 mg/mL. In addition an attempt was made to load the nanoparticles with a widely used pharmaceutical compound and study the respective release kinetics at normal physiological conditions (pH 7.4).

The drug chosen for this part of the work was ibuprofen, $4-Isobutyl-\alpha-methilphenylaceticacid$, a non-steroidal anti-inflammatory drug used for relief of symptoms of pain, fever and inflammation among others.[5]

Overall, this pharmaceutical compound was effectively incorporated both in pure hydrogel and in the ordered mesoporous nanoparticles using different routes. Combining the drug with the hydrogel is already a good platform, but incorporating it into the particles, and dispersing them into the gel is a way to get an even more controlled release.

Contents

1 INTRODUCTION

1.1 The clinical problem

Nowadays, always new chemical compounds are created and tested for medical use. This is allowed thanks to all the technological progresses. The United States Food and Drug Administration (FDA) approved from 22 to 53 new molecular entities each year between 1993 and 1999. Every drug needs a way to be delivered to the site where it is supposed to have its effect. There are already many ways to deliver drugs inside the body, such as tablets, capsules, creams, ointments, liquids, aerosols, injections, and suppositories.[6] Unfortunately, these traditional ways have problems: the chemical substance has to travel into the body before arriving in the right site where it is needed. This happens mostly with systemic delivery ways, e.g. oral and intravenous ones. The longer the path, the more drug will be released in body areas where it should not be released. So this systemic leakage has two negative effects: on one hand, the drug -that spreads where it should not- causes side effects which can be tolerable but also very serious. On the other hand, the amount of drug that gets into the disease site is lower than the initial concentration. Hence, a greater initial concentration is required to have the desired effect in the disease site. Thus, more side effects. There is a parameter which allows to know how much time the drug stays in the body: the **drug elimination half-life** ($t_{\frac{1}{2},elim}$). It can be defined as the time required for the drug concentration to reduce to half its initial value. There are two factors related to this pharmacokinetic parameter: clearance and volume of distribution. The clearance (CL) refers to the rate at which the body eliminates the substance from the body. The volume of distribution (V_d) refers to the distribution of the drug inside the body, i.e. it is the ratio of the amount of drug in the body (administered dose) and its concentration in the plasma.[7] The relationship between these factors is as follows:

$$t_{\frac{1}{2},elim} = \ln(2) \times \frac{V_d}{CL} \tag{1.1}$$

The lower the half-life, the higher the initial dose must be. Plus, ideally, the drug concentration inside the plasma has to be inside the "therapeutic window", i.e. above the minimum therapeutic concentration but at the same time below the

minimum toxic concentration, as the Figure 1.1 shows. Unfortunately, traditional delivery ways do not allow the drug concentration to stay only in this region, but after administration the concentration will go above the minimum toxic level, as a result of the so-called **burst effect**, which is most likely due to the rapid release of surface-associated drug molecules. After this rapid increase, the concentration drops immediately below the minimum therapeutic level. To have a therapeutic effect again, it will be necessary giving a second dose to the patient, which will have the same oscillating behaviour between toxic values and non-therapeutic values.

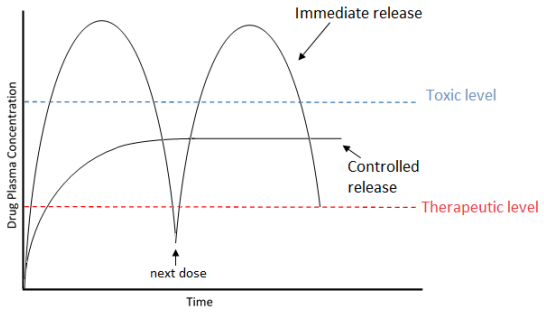

Figure 1.1: Schematic representation of therapeutic and toxic levels in immediate- versus controlled- release dosage form. With the traditional delivery ways the drug concentration in the plasma fluctuates between toxic values and non-therapeutic values. Controlled delivery systems allow to have a concentration that stays in the range of the "therapeutic window".

The great improvement given by controlled delivery drug systems is that it is possible to regulate the drug concentration in the plasma. The ideal trend, shown in the Figure 1.1, stays always in the "therapeutic window", without going in the toxic region, avoiding this way side effects and allowing to gain control of the drug concentration over time.

One of these new controlled delivery systems is based on is the use of nanoparticles (NPs). NPs are tiny materials having size that ranges from 1 to 100 nm. They exist in a very broad variety of different shapes, sizes, structures, properties and they can be for example carbon-based NPs, metal NPs, ceramic NPs, polymeric NPs, lipid NPs, etc.[8]

By smartly combining different types of these nanomaterials with polymers it is possible to develop multifunctional nanomedical platforms for imaging or theraphy. The result is the fabrication of a nanocomposite, defined as a composite in which at least one of the phases shows dimensions in the nanometre range.[9] A nanocomposite has the great benefit of exploiting the advantages of all the materials that compose it, and overcoming the downsides. For example, ceramics have good wear resistance and high thermal and chemical stability, but they are brittle. Polymer materials are widely used in industry due to their ease of production, lightweight

and often ductility, but they have low modulus and strength compared to metals and ceramics.[10] Thus, by combining different materials, improved final properties can be achieved.

In this work a combination of ordered mesoporous nanoparticles and a thermosensitive hydrogel was used, in order to create a new platform that can enable the controlled release of a drug.

1.2 State-of-the Art

1.2.1 Nanoparticles materials for therapeutic applications

Nanotechnology is in a phase of permanent expansion. Its applications extend in many fields: communications, engineering, physics, chemistry, biology, robotics, and medicine[11]. Nanoparticles (NPs) size range (10-1000 nm) is very similar to many proteins and biological macromolecules, as reported in Figure 1.2. Indeed, they showed to be very useful in drug delivery, thanks to their unique features, such as the surface mass ratio, greater than other particles, pore size, shape control, ability to adsorb and carry active compounds, such as drugs.[12,13]

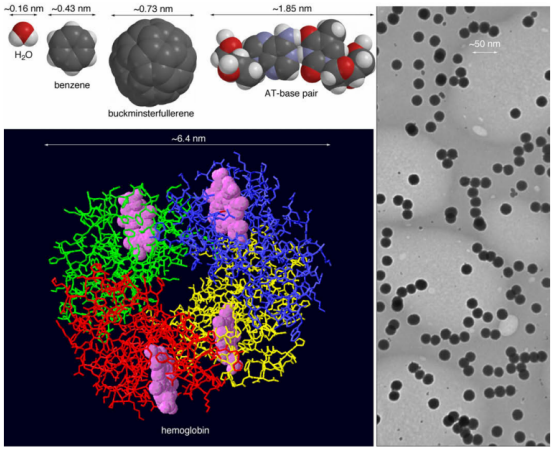

Figure 1.2: Sizes of organic molecules and biological macromolecules (left) in relation to silica nanoparticles (right).[11]

A large variety of NPs have been studied and used for therapeutic applications so far, as shown in Figure 1.3. Frequently used NPs can be classified according to their structure and composition to polymeric, lipid based and inorganic nanoparticles. Polymeric NPs are extensively employed as biomaterials because of their favourable characteristics in terms of simple elaboration and design, good biocompatibility, a broad structural variety and noticeable bio-mimetic properties. Polymeric NPs are usually based on natural polymers such as sodium alginate, albumin, chitosan and gelatin. In addition, several synthetic polymers are also commonly used such as polylactides (PLA), poly (lactide co-glycolides) (PLGA), polyglycolides (PGA), polycaprolactone (PCL), poly (malic acid) (PMLA), polyglutamic acid (PGA), poly (methyl methacrylate) (PMMA), poly (N-vinyl pyrrolidone) (PVP), poly (vinyl alcohol) (PVA), polyacrylamide (PAM), polyethylene glycol (PEG), polyacrylic acid (PAA), poly (methacrylic acid) (PMAA) etc. Liposomes are spherical vesicles which may consist in one or more double layers of phospholipids. They are very similar to micelles, which are made by only one monolayer of lipids. They are very

interesting for the carriage of little biological compunds, like proteins and peptides, due to their high biocompatibility and easy surface modification. Liposomes could carry either hydrophilic drugs -inside the core of the particle, in contact with the hydrophilic heads of the phospholipids- and hydrophobic drugs -between the phospholipid double layers, in contact with the hydrophobic tails. Despite these advantages, liposomes are not used in a large extents in medicine, but rather in the cosmetic industry. Solid lipid nanoparticles were first produced in the early 1990s, and initially used as alternative to liposomes, because they are more stable due to their rigid core, made by hydrophobic lipids that are solid at room and body temperatures, their coating of phospholipids and the use of a large amount of surfactants. They are used a lot since it is possible to tailor their pharmacokinetic parameters and they are less toxic than polymer nanoparticles. Nevertheless, organic nanoparticles have several drawbacks such as low chemical stability, drug release rate that is unsuitable to the specific application, possibility of microbial contamination, as well as undesirable effects of the organic solvents used for particle preparation. Inorganic nanoparticles are non-toxic, hydrophilic, biocompatible and highly stable compared with organic materials. However, less progress has been made in the development of inorganic nanoparticles in drug delivery systems. A special type of such inorganic nanoparticles has been based on carbon nanotubes, a fullerene derivative. Despite an initial huge interest in this type of NPs, nowadays it has diminished due to its possible toxicity.[11] Quantum dots are semiconductor crystals (CdS, PbS, CdSe) with a diameter of a few nanometers. They are mostly used as diagnostic method, due to their optical properties. Indeed, they can be used as fluorescent probes, and the size of the particle determines the color emitted -the smaller the particles the shorter the wavelengths of light. The functionalization of the surface is also possible, allowing an active targeting of particles. However most recently there is a fast growing interest to mesoporous nanoparticles as a result of their robustness, their high loading capacity and the easy chemical functionalization of their surface. This offers a great potential for drug delivery and controlled release of active agents.

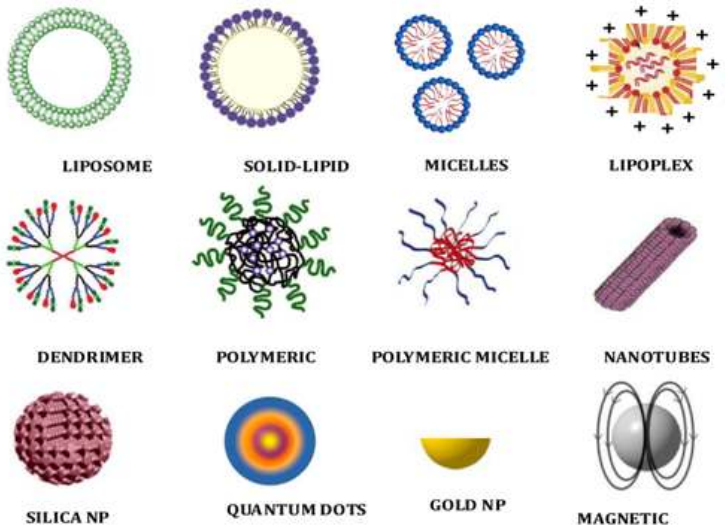

Figure 1.3: Some types of nanoparticles used in biomedical applications.[14]

1.2.2 Hydrogels

Hydrogels are three-dimensional, hydrophilic, polymeric networks capable of absorbing large amounts of water or biological fluids. The hydrogel structure is created by the hydrophilic groups or domains present in a polymeric network upon the hydration in an aqueous environment. The water holding capacity and permeability are the most important characteristic features of a hydrogel. When the contact with water begins, the polar hydrophilic groups are the first to be hydrated, which leads to the formation of primary bound water. Then, the hydrogel swells and it exposes the hydrophobic groups which are also capable of interacting with the water molecules, leading to the so called secondary bound water. Afterwards, the network will absorb additional water, due to the osmotic driving force of the network chains towards infinite dilution.[15]

Due to their high water content, porosity and soft consistency, they closely simulate natural living tissue, more than any other class of synthetic biomaterials. For this reason, they are compatible with biological systems, they can be degradable and responsive to external stimuli. In fact, they can exhibit a significant volume variation in response to small environmental variations, such as pH, ionic strength, temperature, electric field etc. Their highly porous structure is easily tailored and allows drugs loading and their following release with controlled rate.[16]

Biocompatibility is the third most important characteristic property required by hydrogel. Biocompatibility calls for compatibility with the immune system of the hydrogel and its degradation products formed, which also should not be toxic. Generally, hydrogels possess a good biocompatibility since their hydrophilic surface has a low interfacial free energy when in contact with body fluids, which results in a low tendency for proteins and cells to adhere to these surfaces.[15]

There are two main type of hydrogels, the '**reversible**' or '**physical**' gels and the '**permanent**' or '**chemical**' gels. The former type includes gels whose network is made by molecular entanglements and/or secondary forces such as ionic, H-bonding or hydrophobic forces. They are often reversible and it is possible to dissolve them by changing environmental conditions, such as pH, and the ionic strength of solution or temperature. In 'permanent' or 'chemical' gels, the network of covalent bonds that joins different macromolecular chains can be achieved by cross-linking polymers in the dry state or in solution. These gels may be charged or non-charged depending on the nature of functional groups present in their structure. The charged hydrogels usually exhibit changes in swelling upon variations in pH, and it is known that they can undergo changes in shape when exposed to an electric field.

Thanks to their similarity with human body tissue, they are used in many biomedical applications: manufacturing contact lenses, hygiene products, tissue engineering scaffolds, drug delivery systems and wound dressings, pH-sensors, biosensors.[16]

A very common type of hydrogels used in biomedical field is the thermosensitive one: a hydrogel that can modify and alter its properties when the temperature changes. From this point of view, they can be divided into two categories: upper critical gelation temperature (UCGT) hydrogels and lower critical gelation temperature (LCGT) hydrogels, forming a gel by cooling below the UCGT or heating above the LCGT, respectively. The difference can be observed in the phase diagram shown in the Figure 1.4.

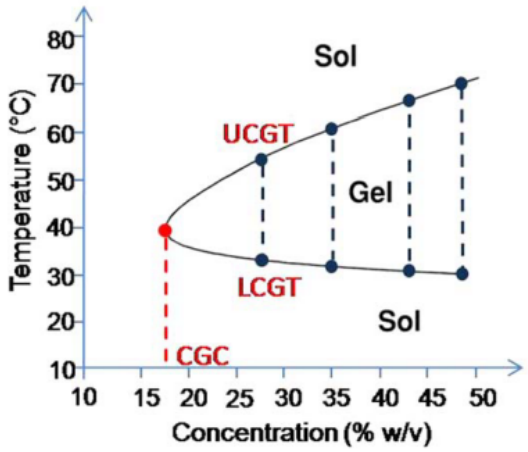

Figure 1.4: Example of a hydrogel phase diagram.[17]

The LCGT hydrogels have become very important since they can be used as carriers for cells, bioactive molecules and drugs due to many advantages, such as:

- the possibility of encapsulating cells and molecules in mild conditions by dispersion in a polymer aqueous solution at low temperature followed by gelation in physiological conditions,
- easy applications, since it is possible to make a minimally invasive injection in the sol state, and then, when the hydrogel is inside the body it turns to gel,
- the ability to assume the desired shape (capability to completely fill body cavities or defects prior to complete gelation).

CHP407: a novel thermosensitive hydrogel

The hydrogel used in this work is the amphiphilic poly(etherurethane) CHP407 with a LCGT behavior. This is practically identical to the polyurethane-based thermosensitive hydrogel NHP407 developed by Monica Boffito et al at Politecnico di Torino[3]. The only difference between NHP407 and CHP407 is in the use of a different chain extender. They are acronyms, where the first letter indicates the chain extender (N is N-BOC serinol and C is CDM), H corresponds to HDI (1,6-hexanediisocyanate), while P407 refers to poloxamer P407. Poloxamers are non-toxic Food and Drug Administration approved poly(ethylene oxide)/poly(propylene oxide)/poly(ethylene oxide) (PEO-PPO-PEO) triblock copolymers, which hydrogels show a LCGT behavior.

Micelle size analysis of the NHP407 system has shown that hydrogel micelles are present in the solutions depending on the solubilized polymer, solution concentration and temperature, and even the size distribution is temperature-sensitive. For example, from the tests carried out by Boffito and coworkers,[3] NHP407 solution with 1% w/V concentration is already completely organized in micelles at 25 °C, and the micelle dimension increases with increasing solution concentration. All the hydrogel tests were made by comparing it with P407, taken as a reference.

The details of the phase diagram of NHP407-based solutions in PBS is shown in Figure 1.5, while the values of the lower critical gelation temperature (LCGT) and upper critical gelation temperature (UCGT) are reported in Table 1.1.

It is clear how the critical gelation concentration (CGC) (see the Figure 1.5) and the LCGT is lower in the NHP407 than the reference polymer.

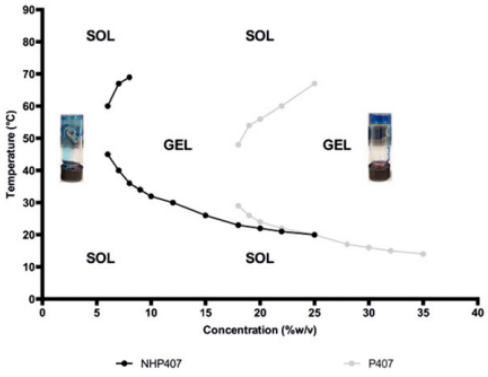

Figure 1.5: Sol-gel-sol transition curves for P407-based (gray) and NHP407-based (black) solutions in PBS obtained by the tube inverting test. The conditions of sol and gel were defined as 'flow liquid sol' and 'no flow solid gel' within 30s, respectively.[3]

The gelation time at 37 °C of NHP407 solutions in PBS was studied as a fundamental parameter for the use of the hydrogels as injectable systems (Figure 1.6).

From 6% w/V concentration to 10% w/V gelation time has a nearly constant decrease, starting from 30 minutes up to 5. Then, it remains constant at 5 minutes until 25 %w/V.

NHP407 solutions with 20% and 25% w/V concentration have the sol-gel transition at the shortest analyzed gelling time: 5 minutes.

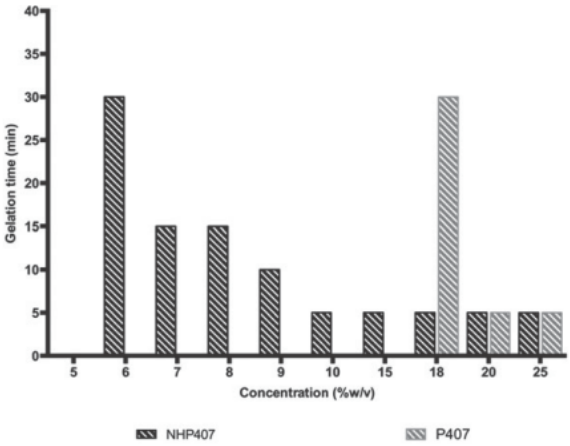

Figure 1.6: Gelation time at 37°C of P407 (gray) and NHP407 (black) solutions.[3]

Another test was made to assess the stability of the hydrogel. The weight change of NHP407 in PBS with 20% w/V concentration was evaluated as function of time at 37 °C: this change gives information about swelling or dissolution phenomena (Figure 1.7a). As the graph shows, P407 progressively loses weight and completely dissolves after 5 days. On the other hand, NHP407 swells the liquid, resulting in a constant increase of the weight, up to 15% after 28 days. PBS absorption in different concentrations of NHP407 is reported in Figure 1.7b , showing that the 20% w/V system is the one that absorbs more PBS, while the 10% w/V one has a decrease in the absorption, and after 20 days it even begins to shrink.

In addition, the shape stability of the formed hydrogels at 37 °C has been qualitatively evaluated injecting P407 and NHP407 solutions prepared at 5 °C into

Table 1.1: LCGT and UCGT values for P407- and NHP407-based solutions in PBS.[3]

		Concentration (% w/V)																	
		5	6	7	8	9	10	12	15	17	18	19	20	22	25	28	30	32	35
P407	LCGT (°C)[a]	-	-	-	-	-	-	-	-	-	29	26	24	22	20	17	16	15	14
	UCGT (°C)[a]	-	-	-	-	-	-	-	-	-	48	54	56	60	67	*b*	*b*	*b*	*b*
NHP407	LCGT (°C)[a]	-	45	41	36	34	32	30	26	c	23	c	22	21	20	c	c	c	c
	UCGT (°C)[a]	-	60	67	69	b	b	b	b	c	b	c	b	b	b	c	c	c	c

[a] Error ±0.5 °C.
[b] UCGT is higher than 70 °C.
[c] Sample not analyzed.

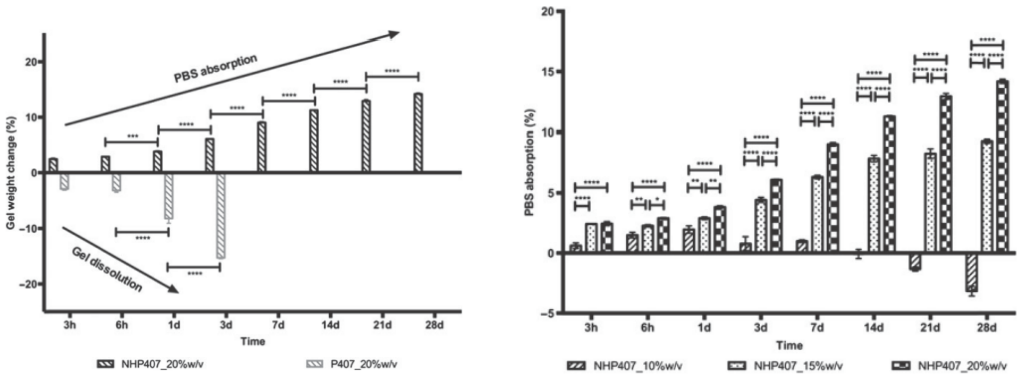

(a) (b)

Figure 1.7: a) Gel weight change(%) as a function of time of NHP407 (black) and P407 (gray). The former has an increase due to the PBS absorption, while the latter has a progressive decrease. b) PBS absorption (%) of different concentrations of NHP407 as function of time. [3]

a water bath kept at 37 °C. Figure 1.8 shows the results for the hydrogels with 20% w/V concentration: the NHP407 hydrogel rapidly formed after injection and assumed a fibrous shape, while the P407 hydrogel showed a tendency to rapidly dissolve in contact with the water medium, as suggested by the light blue color assumed by the water bath.

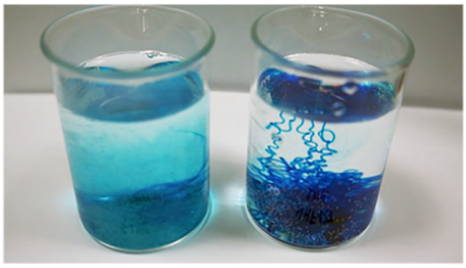

Figure 1.8: Image of injected P407 (left) and NHP407(right) solutions with 20% w/V concentration in water bath kept at 37 °C. The former rapidly dissolves, while the latter forms the hydrogel and assumes a fibrous shape. [3]

1.2.3 Ordered mesoporous nanoparticles

Progress in utilizing inorganic nanoparticles for biomedical applications has advanced rapidly thanks to the extensive amount of work done in the synthesis and modification of these materials. Inorganic particles often exhibit novel physical properties when their size approaches nanometer scale dimensions.

The design of nanoparticles to address diseases and to monitor and protect human health is expected to revolutionize the medical field in the next few decades. In this sense, the capacity of producing nanoparticles in the range of 20–200 nm in diameter has fueled the design of materials large enough to escape clearance through the kidney and small enough to present long circulation times into the bloodstream.

A very attractive approximation concerns the use of nano-sized porous therapeutic carriers since: (1) they can retain the drugs until reaching the targeted site thus not affecting the healthy tissues, (2) the therapeutic efficacy of poor water-soluble drugs might be enhanced by incorporating them into the nanocarriers, (3) nanoparticles can protect the drugs from any possible degradation on their way to their therapeutic target, (4) the surface of the nanoparticles can be functionalised so that they can obtain responsive or targeting properties.[18]

A well-known class of inorganic particles consists of Ordered Mesoporous materials (OMMs), which were first reported in the early 1990s. They had a very quick development since their applications are countless: catalysis, sorption, drug delivery, energy storage and conversion, photonics, and separation to high-tech fields including chips, biotechnology, optoelectronics, sensors, etc.

The synthesis of this type of materials is mostly done with the the so-called nanocasting method using either "soft" or "hard" templates. In general soft-templating is defined as a process in which organic molecules (e.g. surfactants) serve as a 'mold', around which a framework (of an inorganic precursor) is built up. The removal of these organic molecules results in a cavity, i.e. a pore, which retains the same morphology and structure of the organic molecules. The 'soft' templates are usually in the molten or liquid state. Their macroscopic mechanical properties present 'soft' characteristics, such as fluidity under certain conditions. An ample variety of ordered structures can be formed by the soft templating method through the non-covalence intermolecular interaction (short-distance repulsion and long-distance attraction), which is situated between the solid crystal structure and the liquid state structure. Plenty of soft templates, including cationic, anionic and non-ionic surfactants, and mixed surfactant systems, have been utilized to synthesize highly ordered mesoporous materials. During the soft-templating processes, the sol-gel or evaporation induced self-assembly (EISA) processes are typically involved in the synthesis of ordered mesoporous materials. This route is suitable for the preparation of mesoporous silica, because the hydrolysis and condensation rates of silicates can be easily controlled by adjusting reaction parameters such as pH

value and temperature.

The soft-templating method, which can be implemented through two synthetic strategies: cooperative self-assembly and "true" liquid-crystal templating process, of which an explanatory representation is shown in Figure 1.9.[20]

A. In the **cooperative self-assembly process**, there are different forces that can drive the interaction between the inorganic precursor and the surfactants: Coulomb force, covalent bond or hydrogen bonding. The reaction takes place at the interface of the two species, where first of all the inorganic ones polymerize and cross-link and then assemble with surfactants. The process is even influenced by two other factors: the arrangements of surfactants and the charge density between inorganic and organic species. Therefore, in this way different compositions of inorganic–organic hybrids can be formed. The charge density at the surfactant/inorganic species interface governs the assembly process, and after a phase separation and a reorganization finally leads to the formation of ordered 3-D arrangement with the lowest energy.

B. The **"true" liquid-crystal templating process** is based on true or semi-liquid-crystal mesophase micelles produced by high-concentration surfactants as templates. The condensation of inorganic precursors is improved thanks to the confined growth around surfactants. After condensation, the organic templates -the micelles- can be removed.

Despite the great success of the soft-templating method, this is not sufficient enough to prepare many non-siliceous mesostructured materials such as carbon-based, because the non-siliceous precursors are more susceptible to hydrolysis, lack of condensation, redox reactions, weak connection with surfactants or phase transitions accompanied by thermal breakdown of the structural integrity. In this context, hard templating methods are also used for the synthesis of ordered mesoporous materials (mainly carbon-based) involving three main steps: (i) precursor infiltration inside mesochannels of the silica template, (ii) conversion of the precursor in the nanochannels, (iii) removal of the mesoporous silica template, which is well-known.

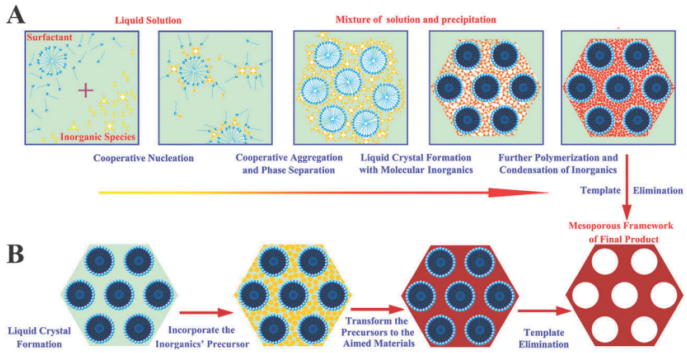

Figure 1.9: Schematic representation of two possible methods for the synthesis of ordered mesoporous materials: A) cooperative self-assembly process and B) "true" liquid-crystal templating process.[20]

Ordered mesoporous silica nanoparticles

The story of OMMs begins in 1992, when researchers at Mobil Oil Corporation developed the first mesoporous material with a hierarchical structure from a family of silicate and alumosilicate solids: the MCM-41 (Mobil Composition of Matter). This was the first time that the term "mesoporous molecular sieves" appeared in a publication.

Before the early 1990s, there has been much desire to develop porous materials with larger pore diameters compared to the zeolite family of molecular sieves, so the diffusional limitations, that restrict the use of large bulky organic substrates, could be overcome.

The main research to expand the pore sizes of zeolites involved the use of small organic additives such as tetramethylammonium hydroxide, tetraethylammonium hydroxide, etc. The use of long chain surfactant molecules such as cetyltrimethylammonium bromide (CTAB), a cationic surfactant opened the way for producing highly ordered silica porous structures with pores transcending into the mesopore regime.

The M41S family of molecular sieves, which includes MCM-41, have a relatively narrow pore size distribution similar to zeolites, but the M41S materials have increased pore diameters compared to zeolites as shown in Figure 1.10.[21]

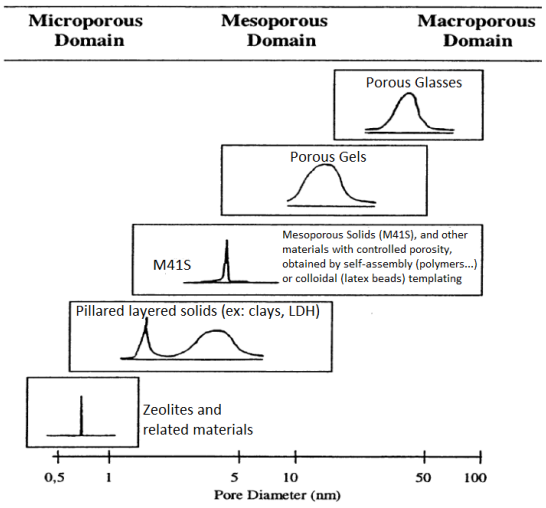

Figure 1.10: Graphical descriptions of the various regions that porous solids occupy with regards to their pore sizes.[21]

MCM-41 consists of a regular arrangement of cylindrical mesopores that form a one-dimensional pore system. A relevant feature is that it is possible to adjust the pore size distribution, because it can be easily tailored modifying the synthesis conditions. MCM-41 presents a pore size distribution centered on presents a mesoporous diameter in the range of 2nm-6.5nm. This narrow pore size distribution,

together with other excellent characteristics such as a high surface area and a large pore volume, are the reason why these materials have attracted so great attention.

MCM-41 synthesis involves the use of surfactants, that form micelles, which are added in order to achieve a defined pore diameter. At the beginning of the process, showed in Figure 1.11, the surfactant micelles are aligned to form rods, which then organize themselves into 2D hexagonal liquid-crystalline structures. Adding the negatively charged silica source, it interacts with surfactant cations under hydrothermal conditions, leading the crystallization and subsequent polymerization of the silica framework around the preformed micellar aggregates and forming a self-assembled mesostructured composite. After surfactant removal by calcinations an ordered mesoporous material is obtained.[22,23]

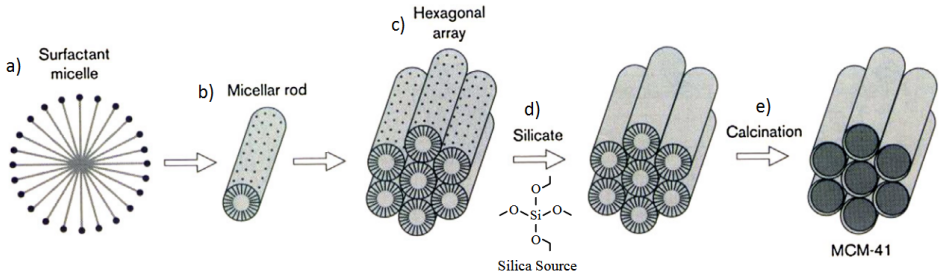

Figure 1.11: Schematic representation of the synthesis process of MCM-41. First of all, a) the surfactant forms the micelles which b) align in rods , and c) subsequently into hexagonal arrays. d) The silica groups cover the organic template that e) will be oxidized and will disappear after the calcination.[22]

Since the MCM-41 presents important features, such as unique mesoporous structure that preserves a level of chemical stability, surface functionality and biocompatibility, it is a suitable candidate as drug vehicle. The mesoporous structure properties, such as pore size and porosity, can be tuned to the size and type of drugs, which represent a great advantage because allows to use MCM-41 as carrier for a lot of different drugs. Another distinctive advantage which make OMS a good drug carrier is that they have well-defined surface properties that allow easy functionalization, useful to control drug loading and release.[24]

Another important type of ordered mesoporous silicas (OMS) is the SBA-15 (Santa Barbara Amorphous). It was developed in 1998 by Zhao et al,[25] and the most important difference between MCM-41 and SBA-15 is that the former is obtained through the basic media route, while the latter is obtained in acidic media. This material has attracted intense interest due to its surface area, well-defined pore structure, inert framework, nontoxicity, high biocompatibility and, the most important difference with the MCM-41, thermal and hydrothermal stability. These very relevant properties allow it to be used in several applications, such as catalysis,

adsorption, chemical sensing, immobilization, drug delivery systems.

Therefore, unlike the MCM-41 it has -beyond higher hydrothermal stability- even larger pore size and thicker pore walls. Furthermore, SBA-15 is obtained from the poly(ethyleneoxide) – poly(propylene oxide) – poly(ethylene oxide) (PEO –PPO–PEO), which is a biodegradable and cheaper polymer than the surfactants used initially in the synthesis of MCM-41.

Also this mesoporous silica has parallel pores and highly ordered hexagonal arrangement. Though it has the benefits of combined micro and mesoporosity and relatively thick silica walls. The micropores, whose representation can be displayed in the Figure 1.12, are created by the penetration of the hydrophobic ethylene oxide chain in the silica walls.

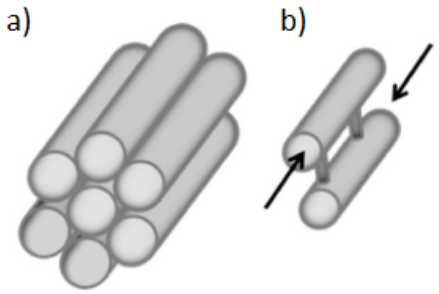

Figure 1.12: a)Schematic representation of the hexagonal arrangement of the mesopores of SBA-15, and b) the microporosity that connect them.[26]

The existence of these micropores interconnecting hexagonally ordered mesopores makes SBA-15 more suitable as a rigid template for the synthesis of other OMMs such as carbons because its inverse replicas retain 3D structures after silica removal due to the existing micropores.[27] The Figure 1.13 clearly shows the problem just described: if the pores of the template were not interconnected, the resulting materials would collapse. As such, SBA-15 was the template used also in this work to synthesize the ordered mesoporous carbon nanoparticles.

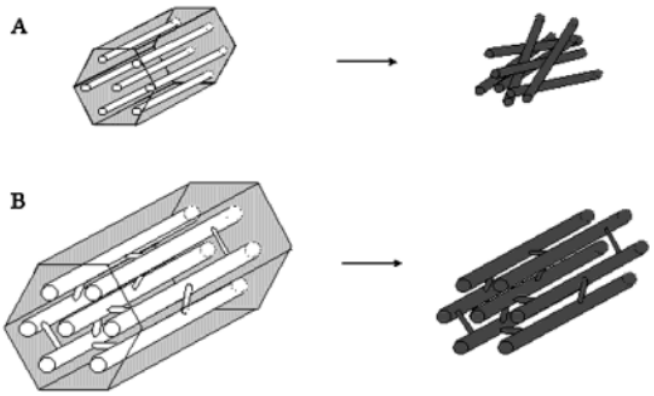

Figure 1.13: Schematic illustration of A) a OMC made with a template which has disconneted mesopores(e.g. MCM-41): the structure collapses. B) OMC made with a template which has conneted mesopores(e.g. SBA-15 calcined at temperatures below about 900 °C).[28]

Ordered mesoporous carbon nanoparticles

The importance and potential of carbon-based materials including the fullerenes, carbon nanotubes, and graphene, are nowadays well known and deeply studied. Though a new type of carbon-based materials is now emerging and has promising applications, highlighted by some highest scientific awards: the ordered mesoporous carbon. Due to its uniform and tunable pore sizes, high specific surface area, thermostability, chemical inertness and biocompatibility, and even periodically arranged monodispersed mesopore space, this type of porous material has attractedstrong interest as also shown by the rapidly increasing number of publications in recent years,[29] as shown in Figure 1.14.

Furthermore, there are a lot of possible structures: 2D hexagonal, lamellar, 3D bicontinuous, body-centered cubic, and a lot of possible forms in which to synthesize them: spheres, rhomb-dodecahedra, wires and ribbons, films, or monoliths.

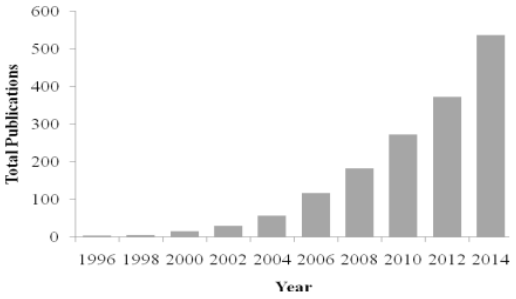

Country/Region	Records	Percentage(%)	Histogram
PEOPLES R CHINA	1544	49.855 %	
USA	411	13.271 %	
SOUTH KOREA	311	10.042 %	
JAPAN	272	8.783 %	
GERMANY	142	4.585 %	
SPAIN	100	3.229 %	
AUSTRALIA	95	3.067 %	
TAIWAN	74	2.389 %	
FRANCE	72	2.325 %	
INDIA	71	2.293 %	

Figure 1.14: Total number of published literature (left) and the main study area distribution (right) with the words "mesoporous carbon" in the title.[29]

OMCs are considered quite advantageous sorbents due to their high specific surface area ($\sim 1500\, m^2 g^{-1}$), large pore volume ($> 1\, cm^3 g^{-1}$), uniform and tailored pore sizes (in the range 3-10 nm), high degree of structural ordering, facile synthesis, high thermal, chemical and mechanical stability, etc.[29 30 31] These materials are also capable of hosting high dispersions of metal nanoparticles and their pore walls can be functionalized with various chemical groups.[30]

The group of novel materials called CMK-n was developed in 1999, when Ryoo et al.[32] described the synthesis of highly ordered mesoporous carbon (CMK-1). They reported the first composition of ordered mesoporous molecular sieves with carbon framework. This first successful preparation of carbon, obtained as the negative of ordered mesoporous silica was an inspiration for scientists to do advanced research on the development of carbon mesostructures. The synthesis of CMK-3 replica was first proposed by Jun et al.[33], who used SBA-15 mesoporous silica as hard template and sucrose as source of carbon.

Depending on the template used, as shown in Figure 1.15, the OMC synthesis can

be differentiated into two categories: hard-templating based and soft-templating based.[29,34]

- **Hard template**: an ordered mesoporous solid template is applied as a mold for the negative replication of OMCs. So the process involves the formation of hard templates such as ordered mesoporous silicas or colloidal crystals, infiltration of the porous template with a carbon precursor and its carbonization followed by removal of the template by etching it in HF or alkaline dissolution. The resulting ordered carbon is an inverse replica of the template used. Pore size control and symmetric ordering are simply determined using the solid template and do not rely on the interaction between the carbon precursor and the template.
- **Soft template**: the advantage is that it is not necessary sacrificing the template by etching it away. It is possible to directly synthesize OMCs by organic-organic self-assembling method using phenolic resin or its derivatives. So there is not the template removal step, which is destructive, and then this is a more simple and scalable method. For this self-assembly method, the cooperative assembly between organic surfactants and carbon precursors usually occurs during evaporation (the so-called **evaporation induced self-assembly, EISA**) or just takes place in solution driven by the hydrogen-bonding (hydrothermal or phase separation). The self-assembly of the composite micelles makes the ordered mesostructure of the carbon.

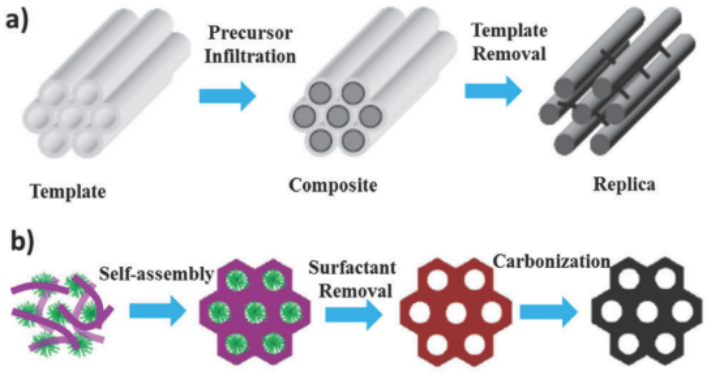

Figure 1.15: Representation of the two synthetis methods of a) hard and b) soft template.[34]

By comparing the two synthesis methods of soft- and hard-templating, it is known that the former allows to makes OMCs with thick pore walls with a continuous framework and thus, offers stability in harsh thermal and oxidation treatments for functionalization. On the other hand, the latter produces OMCs that are much easier to be graphitized.[34]

Functionalization and modification

There are two possible approaches to functionalize OMCs: direct synthesis and post-synthesis reaction. The former can work under a wide range of conditions and it can produce carbons with high loadings and relatively uniform distribution of the functional groups, although its structural ordering seems to deteriorate. The latter shows a high variability in the introduction of functional groups. It is even possible combine the two methods to make multifunctionalized OMCs.

Great efforts have been devoted to the surface functionalization of porous carbon materials in past years. The morphology of the OMCs (including specific surface area, pore size, and volume) can be altered by post-synthesis modification. A series of functional groups can be attached onto the carbon surface through surface oxidation and/or activation, halogenations, sulfonation, grafting through diazonium chemistry, etc. Among them, surface oxidation is one of the most convenient and simplest methods for modifying the carbon surface, with not only attachment of oxygen-containing groups but also alteration of the surface hydrophobic/hydrophilic balance. Indeed, they generally contain a small amount of surface oxygen groups, but it is possible to modify the hydrophobic nature of porous carbons by chemical or thermal treatments to create surface oxygen groups.

The most frequently used method to modify the surface chemistry of carbon materials is oxidation treatments in gas or liquid phase. It is even possible using nitric acid treatment produces the highest concentration of surface oxygen groups, especially carboxylic groups.[29,34]

1.3 Research/Thesis objectives

This work was focused on developing and optimizing a composite hydrogel-based system to allow the sustained release of a drug for non-invasive therapies such as the treatment of non-healing chronic skin wounds. The main challenge was to find an efficient way to combine two inherently different materials, polymers and inorganic nanoparticles, in order to exploit their advantages and thus achieve a good platform for the encapsulation and release of therapeutic compounds. The materials used were the CHP407 hydrogel, an amphiphilic poly(ether)urethane synthesized from poloxamer P407, and two different types of ordered mesoporous materials -silica and carbon-based.

Hydrogels are polymeric materials with a hydrophilic three-dimensional networks capable of holding large amounts of water. They are highly biocompatible, and furthermore, CHP407 is a thermosensitive polymer, with a LCGT behaviour: it has sol-gel transition at 37 °C. Thus, it is a gel at body temperature. On the other hand, ordered mesoporous materials are synthetic materials with a pore diameter between 2 and 50 nm. They have high surface area, usually regular pore frameworks as well as narrow and tailorable pore size distributions. Different types of silica and carbon nanoparticles with average sizes ranging from 100 to 500 nm, were successfully synthesized and characterized using different advanced techniques such as Scanning Electron Microscopy (SEM), Infrared Spectroscopy (IR), Thermal Gravimetric Analysis (TGA), N2 porosimetry, Powder X-ray Diffraction (PXRD).

While silica particles showed no difficulty in being incorporated and well dispersed within the polymer, for carbon particles -due to their hydrophobic nature- it was necessary to test different routes for their incorporation in order to obtain a good dispersion and maximize particles' content into the gel.

All hydrogel-nanoparticles composite systems were characterized in terms of their morphology (through SEM analysis), as well as their gelation (gelation time, tube inverting tests, stability and degradation tests), and rheological properties in an attempt to investigate the effect of the nanoparticles on the hydrogel structure.

As soon as the most promising dispersion protocols were identified, focus was placed on (a) the successful loading of the nanoparticles with a widely used drug such as ibuprofen, (b) the encapsulation of the drug-loaded nanoparticles in hydrogels and (c) the study of the drug release kinetics from the composite systems also in comparison with pure gels. In this context the main aim was to examine the effect of the composition of the hybrid systems on their overall performance in drug delivery processes.

2 EXPERIMENTAL PART

In this work ordered mesoporous particles were chosen as carrier for the drug. Their pores, which have a range size between 2 and 50 nm, according to IUPAC definition, have a definite order in the structure. Furthermore, the goal of this work was to find the proper drug delivery system made not only by the NPs, but even by another vessel which must incorporate the NPs: a thermosensitive hydrogel able to turn in a gel state at 37 ℃, body temperature. The aim of the work was optimizing the protocol to incorporate the NPs into the gel, finding the best type of NPs for the purpose, and maximizing its amount. Indeed, two different concentrations of hydrogel (15%w/V and 20%w/V) and a lot of different types of particles were tested -different by shape, by being or not functionalized, coated or not- all of them are part of two big families: ordered mesoporous silica and ordered mesoporous carbon.

Hence, in order to obtain a platform that ensure a controlled release of the drug, the CHP407 hydrogel -synthesized and kindly provided by Monica Boffito (Politecnico di Torino)- and two different type of ordered mesoporous materials were used in this work. One of them is MCM-41, a silica based material, synthesized during the work, and the other one is the carbon-based material CMK3 -synthesized and kindly provided by Dimitra Giasafaki (NCSR Demokritos).

On these systems few tests were carried out, either on the pure hydrogel (taken as reference) and in the hydrogel with the particles inside, in order to study the particles influence on the gels. Then the samples were observed with SEM to see the structure of the gels and to check the presence and the dispersion of the nanoparticles. After choosing the best combination of hydrogel and particles, and the best protocol, drug release tests were carried out for the pure hydrogel and two type of particles incorporated in the hydrogel: one carbon-based and one silica-based.

The drug chosen for tests was ibuprofen (IBU), a nonsteroidal anti-inflammatory drug (NSAID), generally used as analgesic and antipyretic for a variety of inflammatory pathologies. It can be used either as short duration therapy (e.g. headache) or as chronic therapy (e.g. osteoarthritis and rheumatoid arthritis). It has poor water solubility ($\sim$ 1 mg/mL), so the most common administration way is orally. Although in this way IBU is well absorbed (approximately 100%, with a peak plasma concentration around 1-2 hours after ingestion), it is also rapidly eliminated

from systemic circulation displaying a relatively short half-life (1.7-2 h).[44] Thus, to achieve an extended effect, it is necessary taking several doses. And, although IBU is more tolerated than other NSAIDs –it was the first NSAID to be approved for over-the-counter (OTC) use–it is not totally safe. IBU bad sides appear to be dose and duration dependence, and NSAIDs-related gastric toxicity, including gastric irritation and bleeding, abdominal pain and ulcers have been demonstrated . Nevertheless, these tolerability concerns are associated with higher dose of NSAIDs, and currently do not apply to low-dose, short-term use of IBU for common pain.[?] In order to try to avoid the possible gastric problems, various strategies have been explored, e.g. administration of gastric protectors[?] , use of rectal drug delivery systems[?] , or modified release formulations[?] .

Hence, especially for chronic diseases, which require prolonged drug doses for an extended period, it is very useful have an IBU controlled release, e.g. using NPs as carriers.

2.1 Materials

2.1.1 Synthesis of ordered mesoporous silica materials

The first part of the work focused on producing nanospheres of MCM-41, all of them with the same size of about 100-200 nanometers and all with a spherical shape. Hexadecyltrimethylammonium bromide (CTAB) was used as cationic surfactant, the tetraethyl orthosilicate (TEOS % Aldrich) as source of silica, and the sodium hydroxide as catalyst.

In order to produce 500 milligrams of MCM-41 the following procedure was performed.

A solution of 1 g of the surfactant CTAB, 480 mL of distilled water and 3.5 mL of NaOH 2M was made. This solution was immersed in an oil bath with stirring and heating (Figure 2.1a), then it was left in this way until a stable temperature of 85 °C was reached. Next, 5 ml of TEOS were added dropwise in the 85 °C solution under stirring, giving rise to a white slurry (Figure 2.1b). Then the solution was left in this condition for two hours, in order to allow time for silica particles to settle around the surfactant micelles.

The following step was the filtration of the resulting product and the washing with distilled water. Subsequently, silica particles were allowed to dry at 37 °C. Then they were calcined at 550 °C for 6 hours under air flow of 90 mL per minute, with a heating ramp of 1°C per minute, in order to avoid cracking of the particles during the reaction. During calcination the surfactant decomposes leading to the formation of MCM-41 pores.

2.1.2 Synthesis of ordered mesoporous carbon materials

For the aims of the project, two different types of ordered mesoporous carbons, namely CMK-3 and CMK-1 type were also used. They were both previously prepared at the NCSR "Demokritos" laboratory using a typical hard templating approach[?] . CMK-3 was synthesized starting from the ordered mesoporous silica SBA-15 using the standard hard-templating procedure. The latter was prepared according to a well established method (Zhao et al. 1998[25]; Shin et al. 2001[39]; Lu et al. 2005[40]), using triblock copolymer $EO_{20}PO_{70}EO_{20}$ (Pluronic P123, Aldrich) as the surfactant agent, and tetraethylorthosilicate (TEOS 98 %, Aldrich) as the silica source at a composition of 4 g of P123:0.041 mol TEOS:0.24 mol HCl:6.67 mol H_2O. Aiming to obtain a carbon sample with the inverse structure, SBA-15 was impregnated twice with an acidic sucrose solution, subsequently carbonized by pyrolysis up to 900 °C under N_2 gas flow, followed by etching of the silica framework using HF at room temperature. In a similar approach CMK-1 type spherical carbon nanoparticles were prepared using MCM-48 as starting template. MCM-48 is a cubic periodic silica with interpenetrating network of pores, in contrast to the

(a) (b)

Figure 2.1: Flask with solution of 1 g of CTAB, 480 mL of distilled water and 3.5 mL of NaOH inside the oil bath kept at 85°C, before adding the TEOS (Figure a) and after (Figure b). The images show clearly how the source of silica makes the solution white slurry.

uni-dimensional hexagonal pores of MCM-41.

2.1.3 Synthesis of the CHP407 hydrogel

CHP407 is an amphiphilic poly(ether urethane) synthesized from the Food and Drug Administration approved (PEO-PPO-PEO) triblock copolymer P407. There is an alternative of this polymer, NHP407, in which the only difference is the different chain extender, amino acid derived diol (N-BOC serinol) instead of 1,4-cyclohexanedimethanol (CDM). NHP407 synthesis is carried out as follows, as reported by Boffito et al (2016)[3], although in this work it was kindly provided by Monica Boffito (Politecnico di Torino).

1,6-hexanediisocyanate (HDI) and N-BOC serinol are used as chain extenders, anhydrous 1,2-dichloroethane (DCE) as solvent and P407. First of all, in order to obtain the prepolymer, a solution of P407 in DCE 20 % w/V was made, and then,

HDI aiming at a molar ratio of 1:2 (with respect to P407) was added. The solution was then left this way in presence of the catalyst DBTDL (0.1 %w/V with respect to P407) for 2.5 hours at 80 °C. Next, a solution of N-BOC serinol in DCE 3 %w/V was added, with a molar ratio of 1:1 between N-BOC serinol and P407. After 1.5h at 60°C the reaction was stopped with methanol.

The resulting polymer was collected by precipitation in petroleum ether (4:1 volume ratio with respect to DCE), purified by dissolution in DCE (20 % w/v) followed by precipitation in diethyl ether and methanol (98:2 v:v and 5:1 volume ratio with respect to DCE) and finally washed in diethyl ether (5 g × 100 mL). The polymer obtained was dried overnight under vacuum at room temperature, ground and kept in nitrogen atmosphere at 5 °C.

2.1.4 Embedding ordered mesoporous nanoparticles in hydrogel

Overall, and following intense experimentation, four approaches were used in order to enable not only a good dispersion of ordered mesoporous nanoparticles in the hydrogel solution but also to maximize the amount of particles that can be incorporated. Two concentrations of hydrogel (15% w/V and 20 % w/V) and two types of particles (silica and carbon based) have been used. It should be noted that in all cases the particles were grinded with a mortar before using them. All the gel samples were always prepared in an amount of 1ml, in total, in glass vials (rolled rim bottles, AR glass with PE snap-on lid) with an inner diameter of 18mm at the bottom.

Both OMS and OMC nanoparticles were used to study the different behavior with the hydrogel, placing special emphasis on carbon nanoparticles. Indeed, while the former are hydrophilic, so their encapsulation in gel is simpler, the latter showed complications due to their hydrophobicity. Thus, a wide range of nanoparticles –with different shape, modified or not, coated or not, etc–were tested to study their performance.

- MCM-41: either irregular and spherical silica nanoparticles
- plain CMK3 (irregular carbon nanoparticles)
- functionalized CMK3: two different modifications, realized to make the surface more hydrophilic, were tested. After these processes, the particles' surface presents oxygen groups.
  - particles modified by using H_2O_2 30% w/V for 24h at room temperature
  - particles modified by boiling it in HNO_3 2M for 24h at 120°C
- CSBMAB: carbon particles obtained by a different precursor: it presents nitrogen groups on the surface
- CMK1 spherical nanoparticles
- CMK3 nanoparticles functionalized with a self-immolative polymer (SIP) coating (provided kindly by the group of Prof. M. Vallet, Universidad Complutense de Madrid, Spain)
- CMK-1 nanospheres coated with a self-immolative polymer (SIP)

The Self-Immolative Polymer (SIP) is very useful as a gatekeeper covering the entrance of OMMs pores. Indeed, OMMs presents an open structures made by mesopores very easily accessible. Therefore, using a SIP coated OMM it is possible to somehow close the pores with the cargo inside, and allow to release it only when a

certain stimulus (pH in this case) occurs. This approach leads to stimuli- responsive nanocarriers, that allows to carry and protect the drug until it reaches the desire site in the body, and at the same time, to tailor the release profiles with temporal and dosage control.[19] In this work SIP-coated nanoparticles were used also as a way to achieve a better dispersion of the carbons in the bulk of the hydrogel.

The different routes that were used for encapsulating the nanoparticles in the gel matrix are summarised below.

A. 0.15g or 0.20g of hydrogel (to obtain, respectively, a hydrogel with 15% w/V and 20% w/V concentration) were dissolved in 800μl of distilled water. The solution was vortexed, and left in the refrigerator overnight. In parallel, a second solution was prepared by dispersing a specific amount of particles in distilled water (e.g. 5 mg of particles in 0.5 ml of water) aiming at a concentration of 1mg of particles for each 100μl of water. This solution was also vortexed and subsequently sonicated for a few minutes, in order to obtain a better dispersion. Then 0.2 ml of it were added in the vials with the hydrogel solution.

   With this approach the maximum attained amount of carbon particles in the final hybrid gel system was 2 mg/ml.

B. Variation of A - I: addition of SDS

   Procedure A was slightly modified especially for the case of the carbon-based nanoparticles (due to their hydrophobic character) by pre-dispersing them in an aqueous solution containing 1% w/V of SDS surfactant. The presence of the surfactant did not seem to affect the formation of the gel. The 15% w/V and 20% w/V hydrogel solutions were prepared as described in A. In parallel an SDS aqueous solution was prepared by adding 0.05 g of SDS in 5 ml of distilled water (1% w/V). 5 mg of particles were dispersed in 0.5 ml of this SDS solution. The hydrogel and particle solutions were then mixed as described in A.

   With this approach the maximum attained amount of carbon particles in the final hybrid gel system was 4 mg/ml.

C. Variation of A - II: The particles were pre-dispersed in a larger amount of water reducing at the same time the quantity of the water used for solubilizing the gel.

   10mg of particles were dissolved in 500 µl of distilled water containing 1% w/v of SDS (prepared as described in B). The solution was vortexed and sonicated, and then added in a solution of hydrogel (0.15g and 0.20g) solubilized in 500 µl of water overnight. The same procedure was repeated for 12mg of particles dissolved in 600 µl of distilled water with 1% w/v SDS and added in a solution

of 400 µl of hydrogel. With this method the dispersion was very good in every sample, nevertheless undissolved grains were observed in some cases.

With this approach the maximum attained amount of carbon particles in the final hybrid gel system was 12 mg/ml.

D. Pre-mixing the particles and gel powders

0.15g or 0.20g of hydrogel and the chosen amount of the particles were weighted and put in the same vial, adding 1 ml of distilled water. Then, the solution was vortexed and put into the refrigerator overnight to let the hydrogel solubilize. Once ready, it was sonicated for a few minutes. The particles have been used in amounts of 5mg, 10mg, 20mg. Although the dispersion was very good in every sample, the systems with a hydrogel concentration of 20% have shown some undissolved grains.

With this approach the maximum attained amount of carbon particles in the final hybrid gel system was 20 mg/ml.

Figure 2.2 shows an example of the pure hydrogel, silica and carbon based samples.

Figure 2.2: An example of the samples: pure hydrogel (left), MCM-41 composite (centre), CMK3 composite (right).

At this point it should be noted that the functionalisation or the SIP-coating of the nanoparticles did not seem to have a significant effect on their dispersability in the bulk of the hydrogel. This was clear also through visual inspection, as the formation of aggregates was observed also in these cases. As such it was decided also to test the use of SDS (in procedures B and C) in order to facilitate the wetting of the hydrophobic surface of carbon nanoparticles. SDS is the acronym for sodium dodecyl sulfate, also called sodium lauryl sulfate (SLS), an anionic

surfactant used in many cleaning and hygiene products. It is probably the most studied surfactant among the alkyl sulfates. The formula of this organic compound is $CH_3(CH_2)_{11}SO_4Na$. It has a hydrophobic tail of twelve carbons combined with a polar sulfate head group. This structure, shown in Figure 2.3, reflects its the amphiphilic properties.

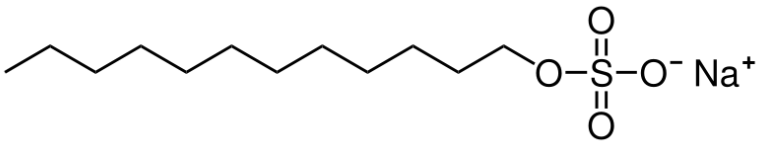

Figure 2.3: SDS molecule. From *Chegg Study website*

There are a lot of studies where SDS was effectively used to achieve a better dispersion of many carbon-based materials, e.g. multi-wall and single-wall carbon nanotubes (MWCNTs and SWCNTs)[?] [?] . The mechanism by which the SDS is able to disperse carbon nanotubes (CNT) is based on hydrophobic/hydrophilic interactions. The hydrophobic tail of the surfactant molecule adsorbs on the CNT surface, while its hydrophilic head associates with water for dissolution.[?] . Another example of the use of SDS is the dispersion of functionalized graphene sheets (FGSs)[?] , from which the CNTs originate.

The problem using a surfactant is that it forms micelles as well as the hydrogel, so it could create issues in the formation of the gel. Nevertheless the influence of SDS on the hydrogels behavior was also studied in previous works. The effect of SDS on the thermal behavior of aqueous hydroxypropylmethylcellulose (HPMC) hydrogels was investigated by J. C. Su et al.[38] They reported that the presence of SDS in a concentration range of 0 mM – 6 mM (so below its CMC) did not significantly affect the gelation of HPMC; the water cages were broken upon heating and sol–gel transition took place owing only to the hydrophobic association of HPMC chains. But with greater concentration of the surfactant the gel formation may be affected.

Another example can be found in Gulyuz and Okay's work[45], where pH responsive physical gels were prepared by micellar copolymerization of hydrophilic monomer acrylic acid (AAc) with large hydrophobic monomer stearyl methacrylate (C18) in solution of different surfactants, including SDS. This study has shown that physical gels with SDS are stable, exhibit high equilibrium swelling ratios and SDS is progressively extracted from the network.

In the present work the addition of SDS did not show to affect significantly the gelation properties of the hybrid gel system as it will be shown below.

2.2 Methods and Techniques

2.2.1 NPs characterization

Ordered mesoporous carbon and silica nanoparticles were characterized after synthesis mainly with Infrared (IR) spectroscopy, N_2 porosimetry, powder X-ray diffraction (PXRD) and scanning electron microscopy (SEM).

N_2 Porosimetry

N_2 porosimetry based on N_2 adsorption/desorption measurements at 77 K, has been generally accepted as the standard method for porous solid or fine powders materials characterization. It exploits the concept of gas adsorption, defined by IUPAC as the enrichment of molecules, atoms or ions in the vicinity of an interface. Physisorption (physical adsorption) occurs whenever a gas (the *adsorptive*) is brought into contact with the surface of a solid (the *adsorbent*). The matter in the adsorbed state is known as the *adsorbate*, as distinct from the adsorptive, which is the gas or vapor to be adsorbed. The forces involved in physisorption are the van-der Waals forces and always include the long-range London dispersion forces and the short-range intermolecular repulsion. These combined forces give rise to nonspecific molecular interactions. Specific interactions come into play when polar molecules are adsorbed on ionic or polar surfaces but, as long as there is no form of chemical bonding, the process is still regarded as physisorption. Physical adsorption processes in porous materials is governed by the interplay between the strength of fluid-wall and fluid-fluid interactions as well as the effects of confined pore space on the state and thermodynamic stability of fluids confined to narrow pores.

However, when the molecules of the adsorptive penetrate the surface layer and enter the structure of the bulk solid, the term absorption can be used. It is indeed difficult to distinguish between absorption and adsorption for sure.[35]

On this basis the surface area and other pore properties of a porous material can be determined by measuring the quantity of an inert gas (e.g. nitrogen) retained on the surface of a sorbent over a wide range of relative pressures (P/Po) and thus the construction of the so-called adsorption isotherm. In practical terms this can be achieved by admitting to the sorbent material successive known volumes of nitrogen and measuring the equilibrium pressure (the gas uptake becomes stable). This is repeated until the partial pressure of nitrogen becomes unity. Similarly, desorption isotherms can be obtained by measuring the quantities of gas removed from the sample as the relative pressure is lowered.

The shape of an adsorption isotherm depends on the interplay between the strength of the fluid–fluid and fluid–wall interactions as well as confined geometry effects, coupled with the state of pore and bulk fluid. IUPAC has classified physisorption isotherms in different types as illustrated in Figure 2.4.

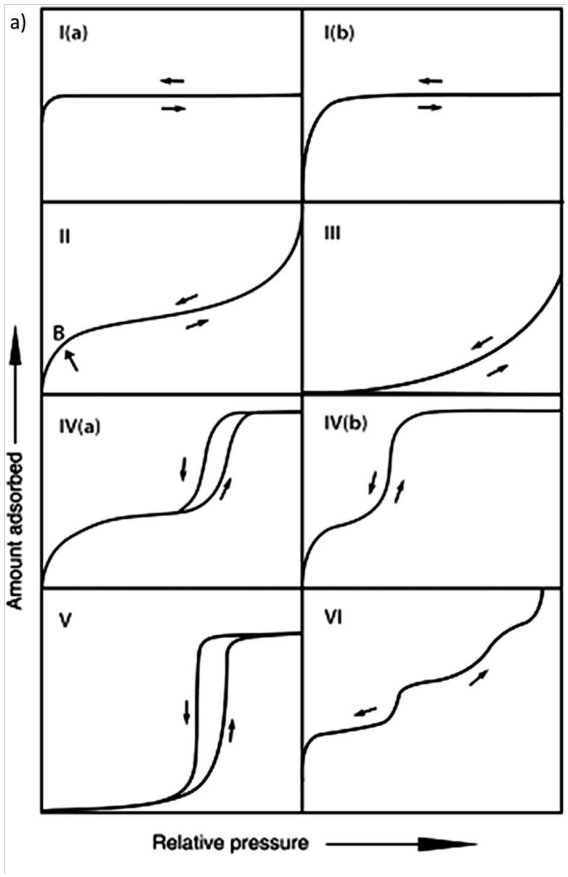

Figure 2.4: The IUPAC classification of adsorption isotherms showing both adsorption and desorption branches.[35]

- Type I or Langmuir isotherms are concave to the P/Po axis and the amount of adsorbate reaches a plateau as relative pressure approaches 1. Type I physisorption isotherms are exhibited by microporous solids (pore size < 2 nm) having relatively small external surfaces (e.g. activated carbons, zeolites etc.). In these cases adsorption is limited to at most only a few molecular layers and as such there is no adsorption after micropores have been filled (and as such the plateau is observed).

- Type II isotherms are the typical form of isotherm obtained on a nonporous or macroporous material (pore size >50 nm), where mono- and then multi-layer formation occurs on the surface. This multilayer formation is also observed in the rare type VI isotherm where each step indicates formation of a new layer of adsorbate on a smooth, non-porous surface.

- Type IV isotherms are associated with the presence of mesopores (pore size

between 2-50 nm), indicated by the steep slope at higher relative pressures.

- Type III and type V isotherms are uncommon; they both indicate very small adsorbed amounts at low pressures are special cases where the interaction between the adsorbate and the adsorbent are relatively weak, i.e., the adsorbate is not completely wetting the surface.

Types I, II and III adsorption isotherms are generally reversible. Types IV and V, associated with mesoporosity, usually exhibit hysteresis between the adsorption and desorption isotherms.

The pore properties of the ordered mesoporous nanoparticles in this work were determined through N_2 adsorption/desorption measurements at 77 K using a volumetric gas adsorption analyser (AUTOSORB-iQ3, Quantachrome Instruments) shown in Figure 2.5.

The sample to analyze has to be placed in a cell, which is connected with gas reservoir (N_2 in this case). Connection between reservoir and cell can be interrupted through a valve. Volume, temperature, pressure of the reservoir are known (called respectively V_r, T_r, P_r), so for the ideal gas law $PV = nRT$ the number of molecules in the reservoir (n_r) can be calculated as follows:

$$n_r = \frac{V_r P_r}{RT_r} \tag{2.1}$$

When the valve is opened the gas inside the reservoir expands and goes into the cell where the sample is placed. Once the gas molecules reach an equilibrium between gas and sorbed phase (gas molecules adsorbed on the sample surface) the number of adsorbed molecules on the sample surface is equal to:

$$n_{sorbed} = n_r - \frac{P_{eq}(V_r + V_s)}{RT_c} \tag{2.2}$$

Where T_c and V_s are respectively cell temperature ($T_c = T_r$) and sample volume, while P_{eq} is the equilibrium pressure. V_s is determined with a calibration method using helium, because its molecules cannot be adsorbed on the surface. Hence, since equation 2.1 is still valid when the valve is closed, when the valve is open with helium flow, the number of molecules n' in the system is:

$$n' = \frac{P_{eq}(V_r + V_s)}{RT_r} \tag{2.3}$$

But, since there are no gas molecules adsorbed, they are in the same number as before the opening of the valve. Then, $n' = n_r$, V_s can be simply calculated.

Prior to the adsorption experiment, it is required to remove all physically adsorbed material from the adsorbent surface while avoiding irreversible changes. Prior to measurement, the samples are appropriately outgassed (e.g. at 250 °C, overnight) under high vacuum (10^{-6} mbar), using ultra-pure N2 (99.999%).

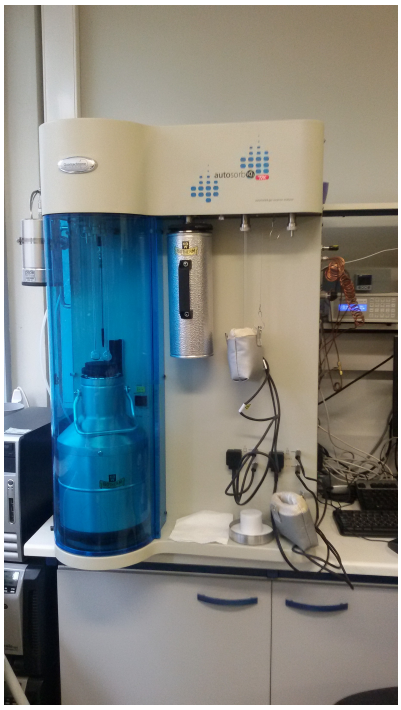

Figure 2.5: N_2 Porosimeter Autosorb iQ_3(Quantachrome Instruments) used during the work.

The pore properties of the studied materials (e.g. surface area, mean pore size, total pore volume, pore size distribution etc.) can be derived by the analysis of the N2 adsorption/desorption data. The standard method applied in physisorption characterization for the determination of the surface area of solid/porous materials is the BET (Brunauer, Emmett, and Teller) method. Usually the evaluation of the BET area involves two steps. First, it is necessary to transform a physisorption isotherm into the 'BET plot' and from it to derive the value of the BET monolayer capacity, nm. The "BET equation" used for this purpose is:

$$\frac{P}{n(P_0 - P)} = \frac{1}{n_m c} + \frac{c-1}{n_m c}\frac{P}{P_0} \tag{2.4}$$

where, n is the weight of gas adsorbed at a relative pressure, P/P_0. The term C, the BET C constant, is related to the energy of adsorption in the first adsorbed layer and consequently its value is an indication of the magnitude of the gas/solid interactions. The BET can be solved graphically through the linear plot of $1/[n(P_0/P) - 1]$ vs P/P_0, which for most solids, using N_2 as adsorbate, is restricted to a limited region of the adsorption isotherm, over the approximate relative pressure range 0.05 - 0.30. The weight of a monolayer of adsorbate n_m can then be obtained from the slope s

and intercept i of the BET plot, where:

$$s = \frac{(C-1)}{n_m C} \tag{2.5}$$

$$i = \frac{1}{n_m C} \tag{2.6}$$

The specific surface area, S, can then be obtained from the monolayer capacity n_m by the application of the simple equation: $S = n_m L s$, where L is the Avogadro constant and s is the cross-sectional area (the average area occupied by each molecule in a completed monolayer). For the hexagonal close-packed nitrogen monolayer at 77 K, the cross-sectional area for nitrogen is 16.2Å. The total pore volume is derived from the amount of vapor adsorbed at a relative pressure close to unity, such as $P/P_0 = 0.95$, by assuming that the pores are then filled with the adsorbate in the bulk liquid state. The volume of nitrogen adsorbed (V_{ads}) can be converted to the volume of liquid nitrogen (V_{liq}) contained in the pores using the following equation:

$$V_{liq} = \frac{P_a V_{ads} V_m}{RT} \tag{2.7}$$

where P_a and T are the ambient pressure and temperature, respectively, and V_m is the molar volume of the liquid adsorbate (34.7 cm^3/mol for nitrogen). The pore volume can be also used to estimate the average pore size as well. For example, assuming cylindrical pore geometry, the average pore radius rp can be expressed as:

$$r_p = \frac{2V_{liq}}{S} \tag{2.8}$$

where V_{liq} is obtained from the previous equation and S is the BET surface area.[?]

Powder XRD

X-ray diffraction (XRD) is a tecnique that can be used to rapidly characterise the crystallinity and composition among others of both solid and powder materials. In this work the XRD patterns were recorded on a Rigaku R-AXIS IV Imaging Plate Detector mounted on a Rigaku RU-H3R Rotating Copper Anode X-ray Generator ($\lambda = 1.54$ Å) shown in Figure 2.6.

When powders are placed in the path of a monochromatic X-ray beam, diffraction will occur from the planes in those crystallites (powder crystals) that are oriented at the correct angle to fulfill the Bragg's law (equation 2.9). The diffracted beams make an angle of 2θ with the incident beam.

$$2d \sin\theta = n\lambda \tag{2.9}$$

Hence, θ and λ are respectively the angle and the wavelength of the incident radiation d is the distance between atomic layers in a crystal, and n is a positive

integer. Figure 2.7a shows a Bragg's law graphic representation. XRD outputs are graphs where the x axis is 2θ, related with the distance d by Bragg's law and the y axis is the intensity. A powder X-ray diffractometer consists of an X-ray source, a sample stage, a detector and a way to vary angle θ. The angle between the sample and the incident X-ray is θ, while the one between reflected X-ray, received by the detector, and the sample is 2θ. θ is increased over time during the analysis, while the detector angle always remains 2θ above the source path. A graphic representation of the instrumentation is reported in Figure 2.7b.

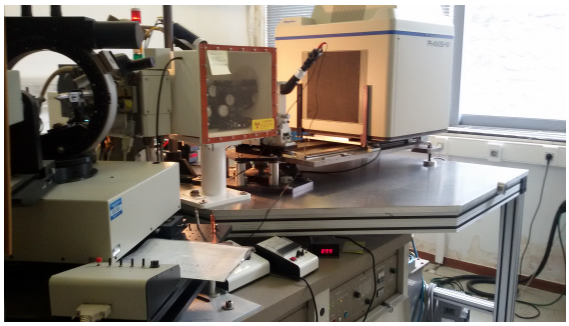

Figure 2.6: Rigaku R-AXIS IV Imaging Plate Detector mounted on a Rigaku RU-H3R Rotating Copper Anode X-ray Generator used during the work.

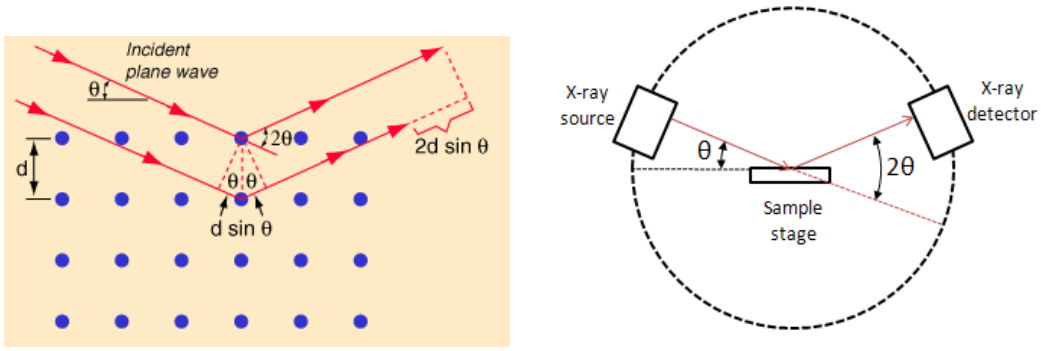

(a) (b)

Figure 2.7: Graphic representation of a) Bragg's law (from *Hyper Physics website - Georgia State University*[41]) and b) powder XRD Instrumentation (from *The Chemistry LibreTexts library*[42])

SEM analysis

The Scanning Electron Microscope (SEM) is used for observation of specimen surface. It is scanned with a focused beam of electrons. The images can be acquired from the detected secondary electrons, which are emitted by inelastic scattering interactions between the specimen and the electron beam. These secondary electrons are detected by a detector, made up of a scintillator (fluorescent substance) with a high voltage (about 10 kV) which attracts them from the specimen. When they hit the scintillator, they generate light which is directed to a photo-multiplier tube (PMT) through a light guide. Then, the light is converted to electrons, and these electrons are amplified as an electric signal. In general, in order to facilitate the acquisition of these electrons, there is also a collector -with few hundred volts applied- placed before the scintillator. In this work Jeol JSM 7401F Field Emission Scanning Electron Microscope (SEM) equipped with Gentle Beam mode was used.

IR spectroscopy

With Infrared (IR) spectroscopy is possible to trigger molecular vibrations through irradiating the sample with infrared light. One of the great advantages of IR spectroscopy is that virtually any sample in virtually any state may be studied.[36] It povides mostly information about the presence or absence of certain functional groups, although without giving detailed information or proof of molecular formula or structure. Therefore, it has to be used in conjunction with other techniques to provide a more complete data of the molecular structure. Infrared radiation is thermal energy with a wavelength between 10^{-6} and 10^{-3} meters, capable of inducing molecular vibrations in covalent bonds. They can vibrate stretching, rocking, and scissoring, but the most useful movement for IR is stretching, because its frequencies produce bands in the IR spectrum. When a sample is exposed to IR light, some frequencies can be absorbed and other transmitted, and some of them can even be reflected. Transmitted frequencies are detected by the detector, obviously carrying information even about the absorbed ones. Therefore, IR spectra plots intensity of the transmission (or absorption) against transmitted (or absorbed) frequencies.

2.2.2 Characterisation of hydrogel/NPs composites

Gelation properties

In order to study the sol-gel transition, a simple tube inverting test was carried out either on pure hydrogel—as reference—and on the hybrid gel system with 10mg and 20mg of plain CMK3 and MCM-41 nanoparticles, prepared mixing the powders, as described in D protocol, set out in the section 2.1.4. The samples (1ml), put in glass vials, were undergone a controlled ramp of temperature from 5°C to 60 °C, in the case of pure hydrogel, and to 40 °C, in the case of the presence of particles, with steps of 1 °C (with an error of ±5 °C). At each step the temperature was maintained stable for 5 minutes, and after that the vials with the samples were inverted and observed for 30 seconds. The conditions of sol and gel were defined by visual inspection as 'flow liquid sol' and 'no flow solid gel', respectively. Figure 2.8 shows the difference of these two conditions in two samples, taken as an example.

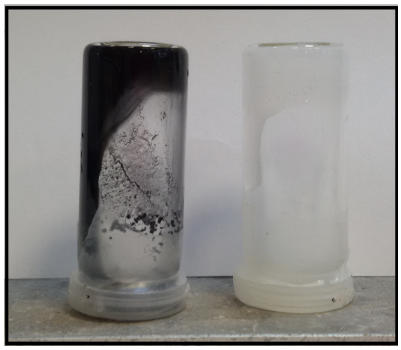

(a)

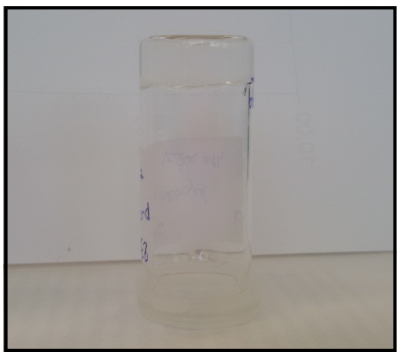

(b)

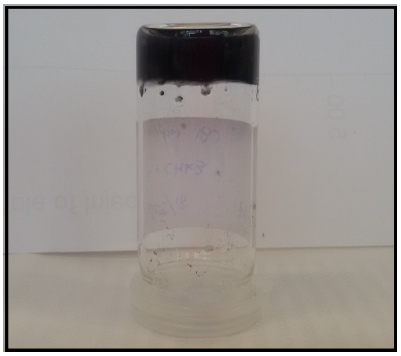

(c)

Figure 2.8: An example of a) CMK3 (left) and MCM-41 (right) samples in a sol condition and b) and c) samples in a gel condition of MCM-41 and CMK3, respectively.

In addition the gelation time at 37 °C was verified for each system. All the samples (1ml), prepared inside glass vials with the protocols described in Section 2.1.4, were incubated at 37 °C for 5 minutes and subsequently inverted and observed

for 30 seconds. The conditions of sol and gel were defined as described above for the tube inverting tests.

Gel stability and dissolution

The gel stability was checked on all the hydrogel/NPs combinations, prepared as described in protocols A and B (described in Section 2.1.4), weighting the samples (1ml) incubated with PBS at specific time intervals: 3 hours, 6 hours, 1 day, 3 days, 7 days. First, the samples in their gel state were weighted to know their initial weight (w_i). Thus, 1ml of PBS was added in each vial and the samples were kept in the oven at 37°C and taken out only at the specific time intervals to be weighted (w_f). At each time interval, the excess of PBS was removed from the vial, the sample was weighted, and another 1 ml of PBS was added. Therefore, the PBS absorption was estimated according to the following formula:

$$PBS\,absorption\,(\%) = \frac{(w_f - w_i)}{w_f} \times 100 \tag{2.10}$$

All the samples were treated together with a reference of pure hydrogel sample (one for each concentration , 15% and 20% w/v) to make sure that differences in environmental conditions (humidity, temperature, etc.) did not have any effect on the trends. In this way the sample and the respective reference were influenced in the same way and the values could be compared.

After seven days of incubation with PBS the gels were freeze dried and then weighted again ($w_{freeze\,dried\_f}$). The initial weights ($w_{freeze\,dried\_i}$) were estimated considering the weight of the material without the addition of the solvent. Gel dissolution was estimated according to:

$$Hydrogel\,dissolution\,(\%) = \frac{(w_{freeze\,dried\_i} - w_{freeze\,dried\_f})}{w_{freeze\,dried\_i}} \times 100 \tag{2.11}$$

Morphology

The surface morphology and particles dispersion was evaluated with SEM images in the followings samples, after lyophilization:

- hydrogel 15% w/V with 20mg/ml of MCM41 (1ml) synthesized following protocol D reported in section 2.1.4
- hydrogel 15% w/V with 20mg/ml of CMK3 and CMK1 (0.5ml) synthesized as follows: a solution with 75mg of polymer in 400μl of demineralized water was left overnight to solubilize. Then a particle suspension (sonicated with probe sonicator at 20% amplitude, for 3 minutes) with a concentration of 100 mg/ml

in demineralized water containing SDS at 1%w/V was prepared, and then100μl of it were added to the polymer solution to reach a final polymer and particle concentration of 15%w/V and 20mg/ml. The synthesis and SEM images of these two samples were kindly performed by Monica Boffito (Politecnico di Torino).

2.3 Drug incorporation

Following the synthesis of the nanoparticles and the identification of the most effective protocols for their encapsulation in the hydrogel matrix, the next step was to incorporate an active therapeutic compound in both the pure hydrogel and NPs. Ibuprofen (IBU) has been loaded into the pure hydrogel by (a) pre-dispersing it in an organic solvent -being a hydrophobic drug-, or (b) simply mixing it with the hydrogel powder before solubilisation. On the down side, in the former case the organic solvent -ethanol- can damage the polymer, and in the latter the drug can remain undissolved in the sample. As such there were unavoidably limitations regarding the amount of drug that could be directly incorporated in the hydrogel matrix with either way.

On the other hand, the drug was successfully loaded into silica and carbon nanoparticles in a large amount - 1:1 w/w ratio. This significant loading degree was achieved with a melt infiltration technique, which was proven to be much faster and more effective than the conventional solvent-based method. The choice of the melt-inflitration route was based on the appropriate IBU melting. First of all, particles and drug powders were mixed together to form a physical mixture with a 1:1 weight ratio, aiming to fully occupy the total pore volume of the nanoparticles as this was determined by pore analysis (N_2 porosimetry measurments). Then, keeping the powders in a water bath at 87 °C -so above the IBU melting poiting (76°C)- and under stirring for 30 minutes, the drug melts and infiltrates the particles' pores. This procedure was implemented with a rotovapor RII (Duchi) as shown in Figure 2.9.

Subsequently, the powders were kept in an ice bath for 10 minutes to induce the solidification of IBU (Figure 2.10).

In order to check if the drug was really inside the pores and not on the external surface of the particles, the IBU loaded powders were analyzed with Thermogravimetric Analysis (TGA). It is used in the research and development of various substances and materials - solid or liquid – in order to study their thermal stability and composition. It is a technique in which the mass of a substance is monitored as a function of temperature and time as the sample specimen is subjected to a controlled temperature program under a defined and controlled environment -heating rate, gas atmosphere, flow rate, crucible type, etc-. A TGA apparatus consists of a precision balance that carries the crucible where the sample can be placed. It is encased in a furnace and is heated or cooled during the experiment, under a constant flow of gas -inert or reactive, depending on the analysis. The mass of the sample is constantly monitored during the experiment.

In this work a SETSYS Evolution (Setaram Instrumentation), shown in Figure 2.13a, was used, which is a special device which also allows to do Differential Scanning Calorimetry (DSC) analysis and thus qualify and/or quantify the heat effects occurring during a mass variation or any transition not related to a mass change.

The IBU loaded silica (MCM-41) and carbon (CMK3 and CMK1) nanoparticles were then embedded in hydrogel matrices. Different approaches were tested to study the influence of various parameters (amount of NPs and thus drug, encapsulation mode) as described below. In all cases a hydrogel concentration of 15% w/V (1ml) was used, samples were prepared in triplicate and physiological solution (0.9%w/V NaCl, pH 5) was used, instead of water, to solubilize the hydrogel. The procedures that were followed for the incorporation of IBU in the gel matrices by either directly mixing pure drug with pure hydrogel before solubilization or through the embedment of drug loaded nanoparticles are described below.

For the incorporation of ibuprofen in pure hydrogel:

I. A typical protocol was initially followed by pre-dispersing the drug in ethanol - the solution was prepared by mixing 20 mg of IBU and 0.5 ml of ethanol (final concentration 40mg/ml, matching IBU solubility in this organic solvent). In a next step a small amount of this solution (to prevent the degradation of the gel due to ethanol) was added to the hydrogel before the solubilization step. More specifically two different samples were prepared by either adding 15µl or 25 µl of this solution. The IBU content of the drug loaded hydrogels prepared in this way was estimated to be about 0.6 and 1 mg IBU/ml, respectively.

II. As the above protocol did not allow to incorporate increased amounts of drug into the hydrogel (due to the presence of ethanol), an attempt was made to directly mix 1 or 2mg of drug with the hydrogel powder before solubilization. For this purpose SDS was also added in the physiological solution (again at a 1% w/v concentration), to improve the wetting of the drug this time as ibuprofen is poorly soluble in water. The IBU content of the pure hydrogel samples prepared in this way were estimated to be approximately 1 and 2 mg IBU/ml, respectively (avoiding though the addition of ethanol).

On the other hand the protocols described in Section 2.1.4 were used for the incorporation of the drug loaded NPs in pure hydrogel, aiming at different particle (and thus drug) loading. In brief:

III. 2 mg of IBU loaded CMK3, CMK1 and MCM-41 NPs were combined with the hydrogel using blending protocol B as described in Section 2.1.4. In this way the targeted initial drug loading of the composite gel system was approximately 1 mg IBU/ml.

IV. 4 mg of IBU loaded CMK3, CMK1 and MCM-41 NPs were combined with the hydrogel using again blending protocol B. In this way the targeted initial drug loading of the composite gel system was approximately 2 mg IBU/ml.

V. 20 mg of IBU loaded CMK3 and MCM-41 NPs were combined with the hydrogel using blending protocol D as described in Section 2.1.4. In this way the

targeted initial drug loading of the composite gel system was approximately 10 mg IBU/ml.

2.4 Drug release tests

All the IBU loaded samples -pure hydrogel and composite systems-, after their preparation were left for 15 minutes at 37 °C to induce gelation inside an incubator (LabTech), shown in Figure 2.13b. Then 1ml of PBS (kept at 37 °C) was added (always keeping samples in the incubator at 37 °C, without shaking). The release medium was collected and refreshed after 3h, 24h, 3d, 5d, 7d, 10d, 14d, 21d. At each time steps 1ml of fresh PBS was added in the vials. Ideally, the sampling should aim to simulate body environment: when a nanocomposite is inside the body and it releases drugs or other molecules in the disease site, the blood has a continuous diluent action. So the extracts should be collected very often, but the problem with gels is that, taking them out of their 37 °C environment (incubator showed in Figure 2.13b) means to submit them to a too frequent temperature change. Then, these time points were a compromise between blood action simulation and the stability of gels.

IBU concentration in the samples was determined by UV analysis taking the maximum absorbance at 222 nm.

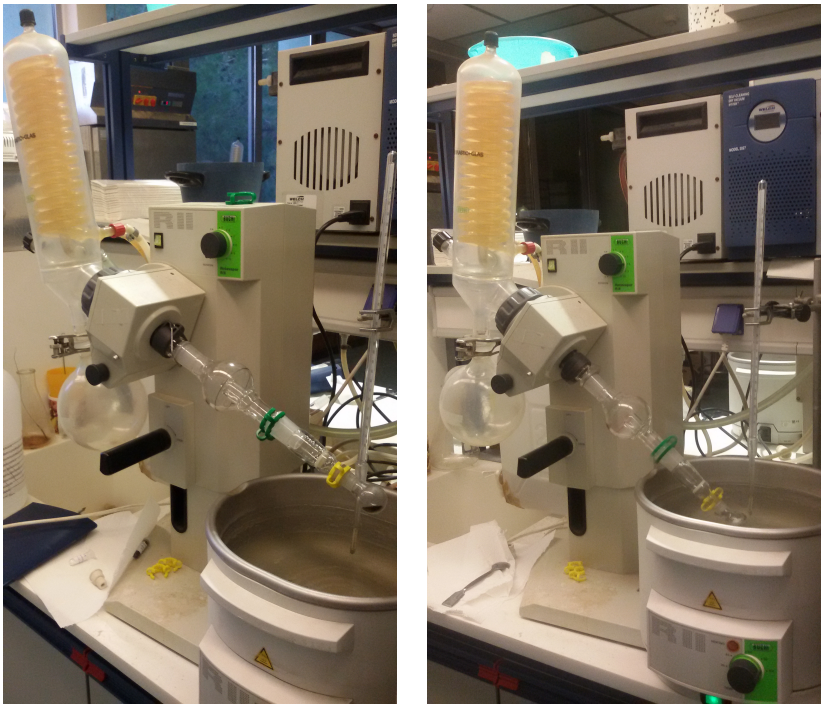

(a) (b)

Figure 2.9: IBU loading into the ordered mesoporous nanoparticles by melt infiltration. CMK3 nanoparticles are shown on the left -outside the water bath used to keep the powders at 87°C- and MCM-41 nanoparticles are shown on the right- already inside the water bath.

Figure 2.10: After the IBU melting procedure, the produced drug loaded powder was left in an ice bath for 10 minutes to allow the solidification.

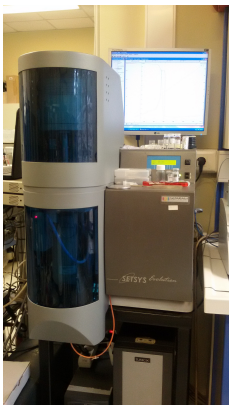

Figure 2.11: Thermogravimetric Analysis (TGA) used during the work.

Figure 2.12: Incubator used during the drug release tests to keep the samples and PBS at 37°C.

(a) (b)

Figure 2.13: a) Thermogravimetric Analysis (TGA) used during the work and b) Incubator used during the drug release tests to keep the samples and PBS at 37°C.

3 RESULTS AND DISCUSSION

3.1 Nanoparticles properties

Two important features of nanoparticles used for therapeutic applications are that (a) they must have a submicron ($<$ 1 um) size, preferably around 100-200 nm and for rigid particles (b) they must have an as regular as possible shape (preferably spherical)[49]. The SEM images in Figures 3.1a and 3.1b show how these two goals have been achieved with the materials that have been used in the present work: MCM-41 silica and CMK1 carbon particles have a regular spherical shape and uniform size around 100 nm. Figure 3.1c shows the typical cylindrical, rod-like shape of CMK3 nanoparticles, with average size 500 nm.

Regarding their surface properties, the FTIR spectra of MCM-41 and a representative carbon sample (CMK3 type) over the range 4000–400 cm^{-1} are presented in Figure 3.2: they are in agreement with literature for these types of materials. MCM-41 pattern exhibits several signals; the strong and sharp peaks at about 1100 cm^{-1} and 790 cm^{-1} are characteristic bands of Si—O—Si moieties in the framework structures, corresponding to asymmetrical and symmetrical stretching, respectively. On the other hand the CMK3 pattern is practically featureless indicating the absence of dominant functional groups from the surface of the carbon material.

The PXRD pattern of MCM-41 (Figure 3.3a) exhibited the typical pattern of the 2D hexagonal strutcture[46,47]. It showed four distinguishable peaks: a strong peak at 2.32° which corresponds to (10) diffraction and three weaker peaks at 4.02°, 4.63° and 6.11° that can be assigned to (11), (20) and (21) diffractions respectively, indicating a well-defined hexagonally ordered mesoporous structure. The same big peak plus other two smaller peaks can be observed in the CMK3 PXRD pattern (Figure 3.3b), since it has the same 2D hexagonal structure. Thus it declares the highly ordered arrangement of the amorphous carbon nanorods. The first peak at 1.07° corresponds to (10) diffraction and two peaks at 1.81° and at 3.44° corresponds to (11) and (20) diffractions, respectively.

CMK1 low angles PXRD pattern (Figure 3.3c) gives other information, since

it present a cubic 3D structure[48]. One strong peak at 1.81°, assigned to (110) diffraction, and a smaller one at 3.14° assigned to (211), indicates a 3D cubic space lattice.

The nitrogen sorption isotherms of the powder materials MCM-41, CMK3 and CMK1 at 77 K are illustrated in Figure 3.4. They are plotted as the quantity of gas adsorbed $[cm^3/g]$ against the equilibrium relative pressure (p/p_0), where p_0 is the vapour pressure of nitrogen at 77 K. The N_2 adsorption isotherms for all samples are of type IV (based on IUPAC classification[35]), typical of mesoporous materials. Type IV isotherms are characterized by an initial monolayer-multilayer adsorption on the mesopore walls ($p/p_0 < 0.01$), followed by a condensation step, and a final saturation plateau, of variable length (even reduced to only few inflexion points, like in the case of CMK1). The phenomenon of pore condensation takes place when a gas condenses to a liquid-like phase in a pore at a pressure $p < p_0$. CMK1 shows no well-defined condensation steps, but only a slow increase at $p/p_0 < 0.4$, indicating presence of pores of different size. At low relative pressures ($p/p_0 < 0.01$), all samples reveal enhanced N2 adsorption, indicating a significant amount of microporosity.

In all cases significant meso- to macro-porosity was also evident at high relative pressures where a significant increase of the adsorbed amount of nitrogen is observed. This phenomenon, which is more pronounced with the order MCM-41 > CMK1 > CMK3, is attributed to the pore space created by the packing of the nanoparticles.

The analysis of the above N_2 adsorption isotherms allowed to determine the pore properties of the three types of nanoparticles, which are presented in Table 3.1. The calculations were done with the help of the special AsiQWin software developed by Quantachrome. The specific surface area values were calculated by the Brunauer-Emmett-Teller (BET) method, as described in Section 2.2.1. The samples showed to have an average pore size between 4-5 nm in all cases and a large BET area, $\sim 1000 m^2/g$ for MCM-41 and CMK3 and even $\sim 2000\ m^2/g$ for CMK1. The total pore volume was estimated at $p/p_0 \approx 0.96$ and all the samples showed to have a large total pore volume ($\sim 1-2\ cm^3/g$) showing a good potential for increased drug loading.

Table 3.1: Structural parameters of MCM-41, CMK3 and CMK1.

	S_{BET} $[m^2/g]$	TPV $[cm^3/g]$	Pore width [nm]
MCM-41	1081	1.0	4
CMK3	1236	1.2	5
CMK1	1911	1.8	4

S_{BET}:Brunauer–Emmet–Teller (BET) specific surface area.

TPV: Total pore volume calculated at a relative pressure of 0.96.

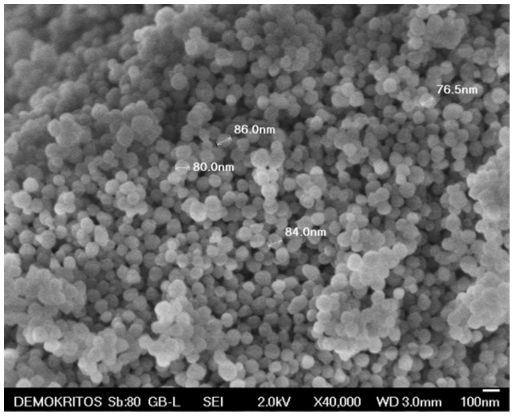

(a)

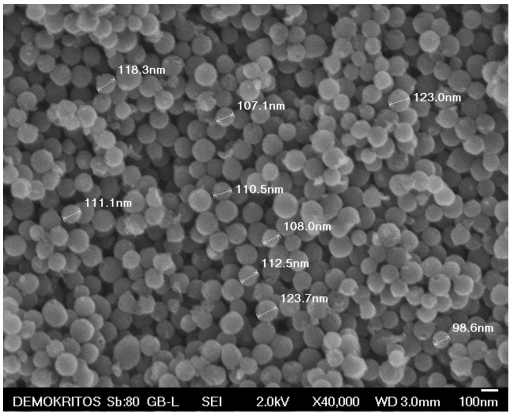

(b)

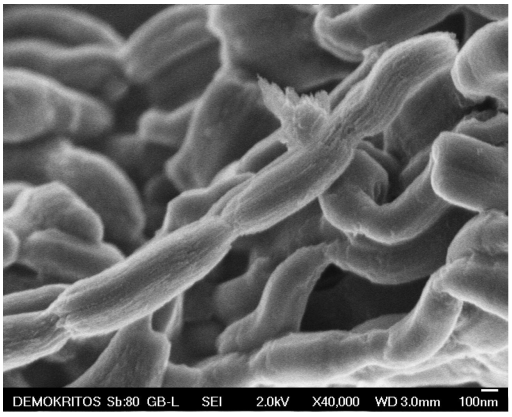

(c)

Figure 3.1: SEM images of a) MCM-41, b) CMK1 and c) CMK3 particles after the synthesis.

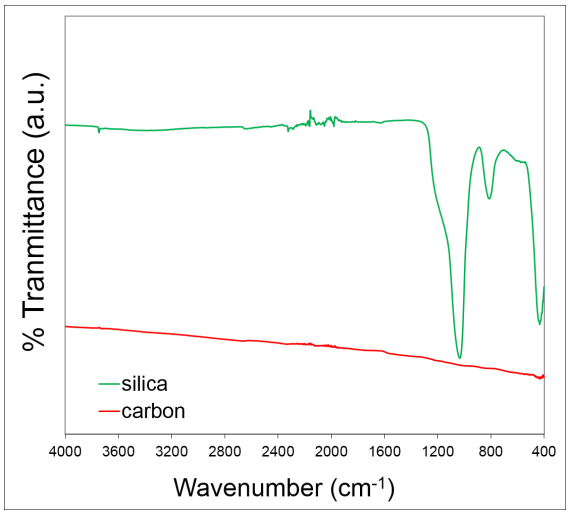

Figure 3.2: FTIR results of MCM-41 (green line) and CMK3 (red line).

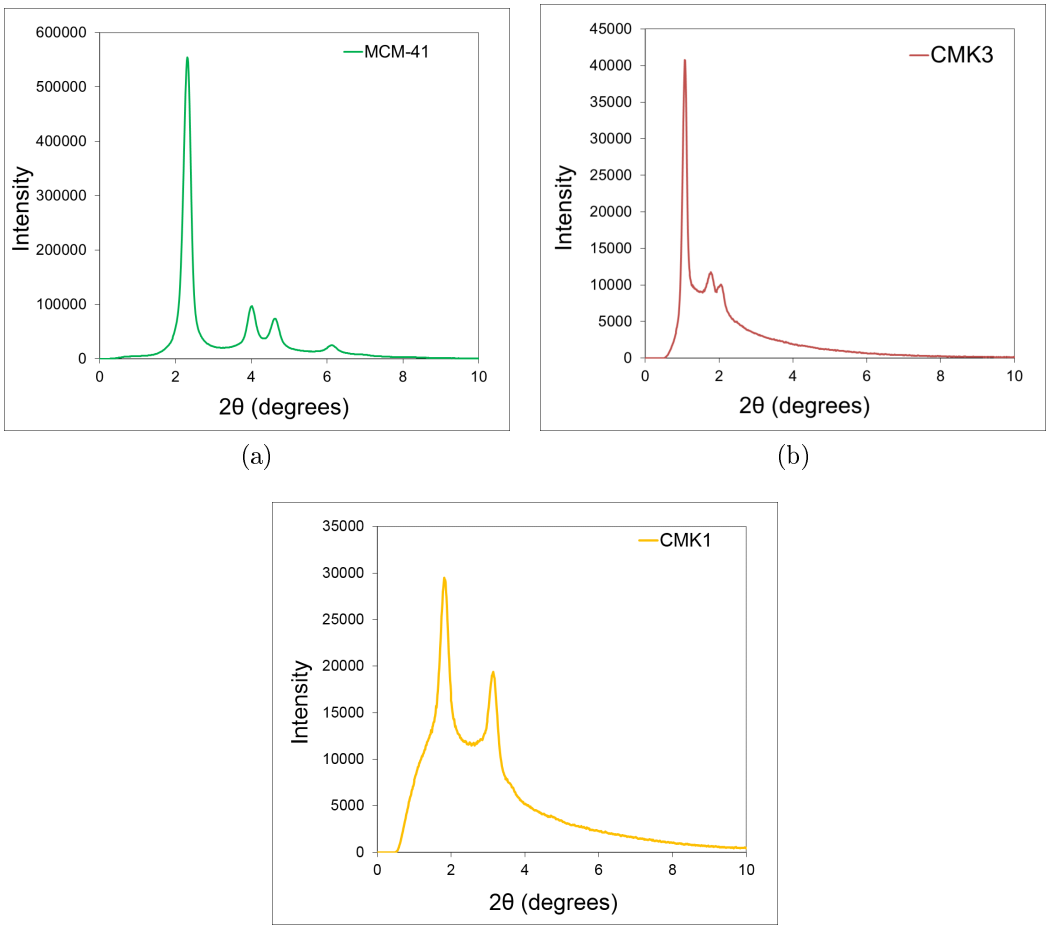

(a) (b) (c)

Figure 3.3: Small angle PXRD patterns of a) MCM-41, b) CMK3 and c)CMK1.

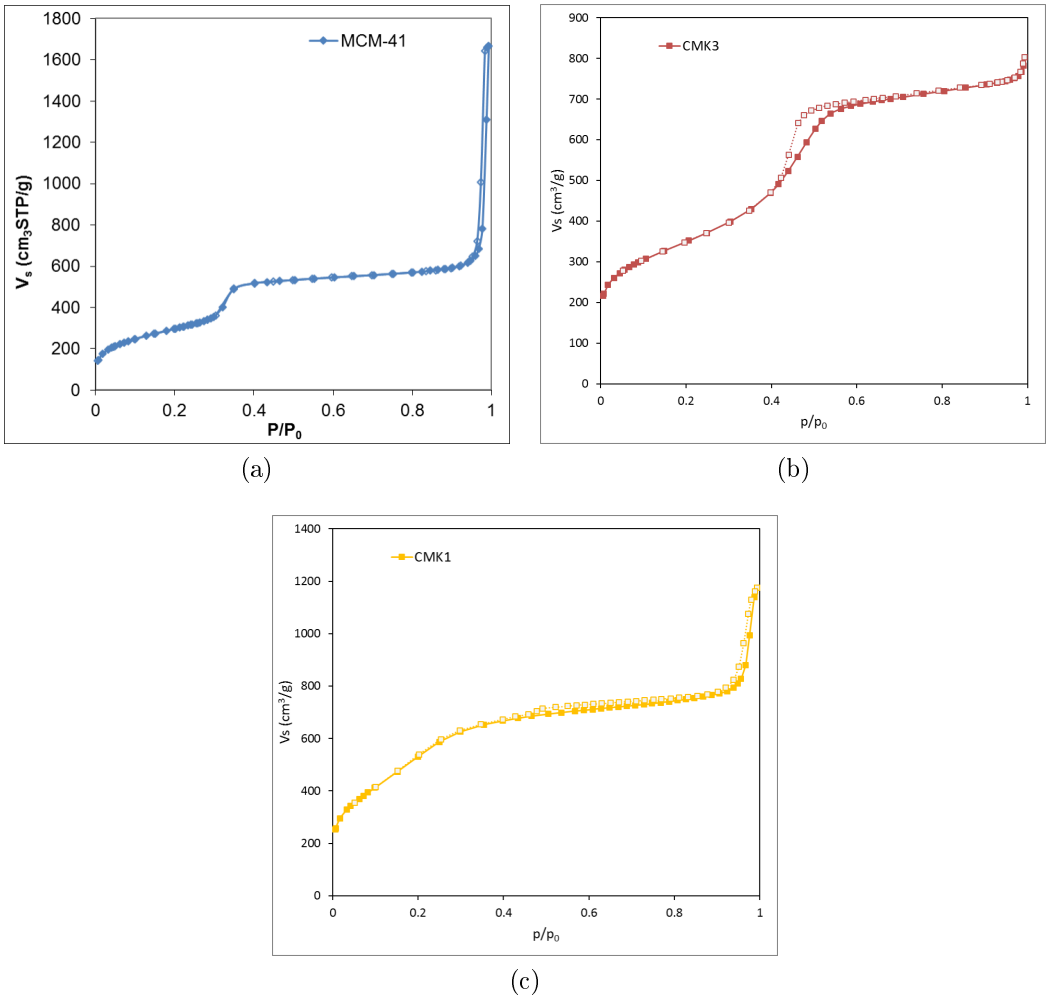

Figure 3.4: N_2 sorption–desorption isotherms at 77 K of the a) MCM-41, b) CMK3 and c) CMK1 (*full symbols/ continuous line*: sorption, *empty symbols/dashed line*: desorption).

3.2 Gelation properties of composite systems

Tube inverting tests, gelation time and stability and degradation tests allowed to study the sol-gel transition in both the pure and composite gel systems and to verify that the presence of the nanoparticles does not influence the gel formation, or at least not to a large extent. All the systems showed to turn into gel at 37 °C within 5 minutes. The results of tube inverting tests are reported in Table 3.2.

Table 3.2: LCGT values for pure hydrogels and composite systems with hydrogel and NPs.

	amount of NPs	Concentration (% w/V)	
		15	20
pure hydrogel	-	26 °C	22 °C
hydrogel + CMK3	10 mg	25 °C	20 °C
	20 mg	26 °C	*
hydrogel + MCM41	10 mg	25 °C	20 °C
	20 mg	26 °C	*

* Sample not analyzed.

The presence of particles affects the formation of the gel in a very minimal extent. Indeed, Table 3.2 shows that the LCGT changes only of one -for 15% w/V samples- or two degrees -for 20% w/V samples.

Figures 3.5 and 3.6 show stability tests results for all the systems tested. The trend in the composite systems with the particles follows in all the cases the trend of pure hydrogel, so the polymer absorbs PBS and swells even with the presence of particles. Thus, this test provides further evidence of how hydrogel behavior is not affected by particles. Slightly better behavior occurs in systems with SDS, in terms of similarity with the pure hydrogel. Furthermore, samples with 20% w/V polymer concentration showed to have a greater PBS uptake than 15% w/V samples. Also from the dissolution tests (Figure 3.7)it is clear that the hydrogel is not affected to a large extent from the NPs presence. Only two composite systems showed to have a greater dissolution than the pure hydrogel -CSBMAB (with nitrogen groups on the surface) and CMK3 modified withH_2O_2 (with oxygen groups on the surface). All systems with 15% w/V concentration of polymer showed a greater dissolution than 20% w/V systems.

In addition, it should be noted that the usrface functionalisation does not facilitate the dispersion and just the presence of the surfactant (SDS) is sufficient.

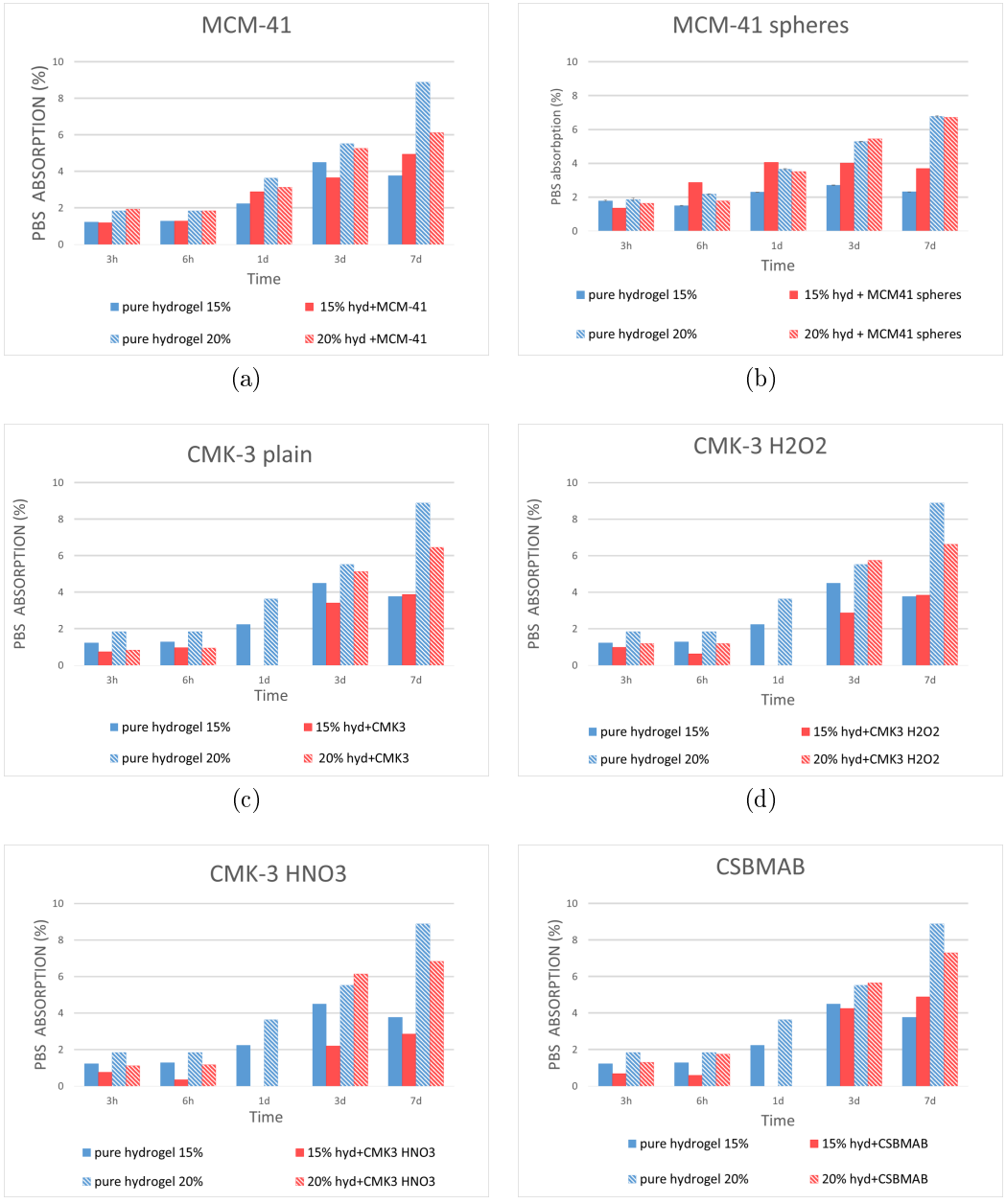

Figure 3.5: PBS absorption (%) in systems with (a) MCM-41 irregular particles, (b) MCM-41 spherical particles, (c) CMK3 plain, (d) CMK3 modified with H_2O_2, (e) CMK3 modified with HNO_3 and (f) carbon particles obtained with a different precursor. In all systems the particles concentration is 2 mg/ml.

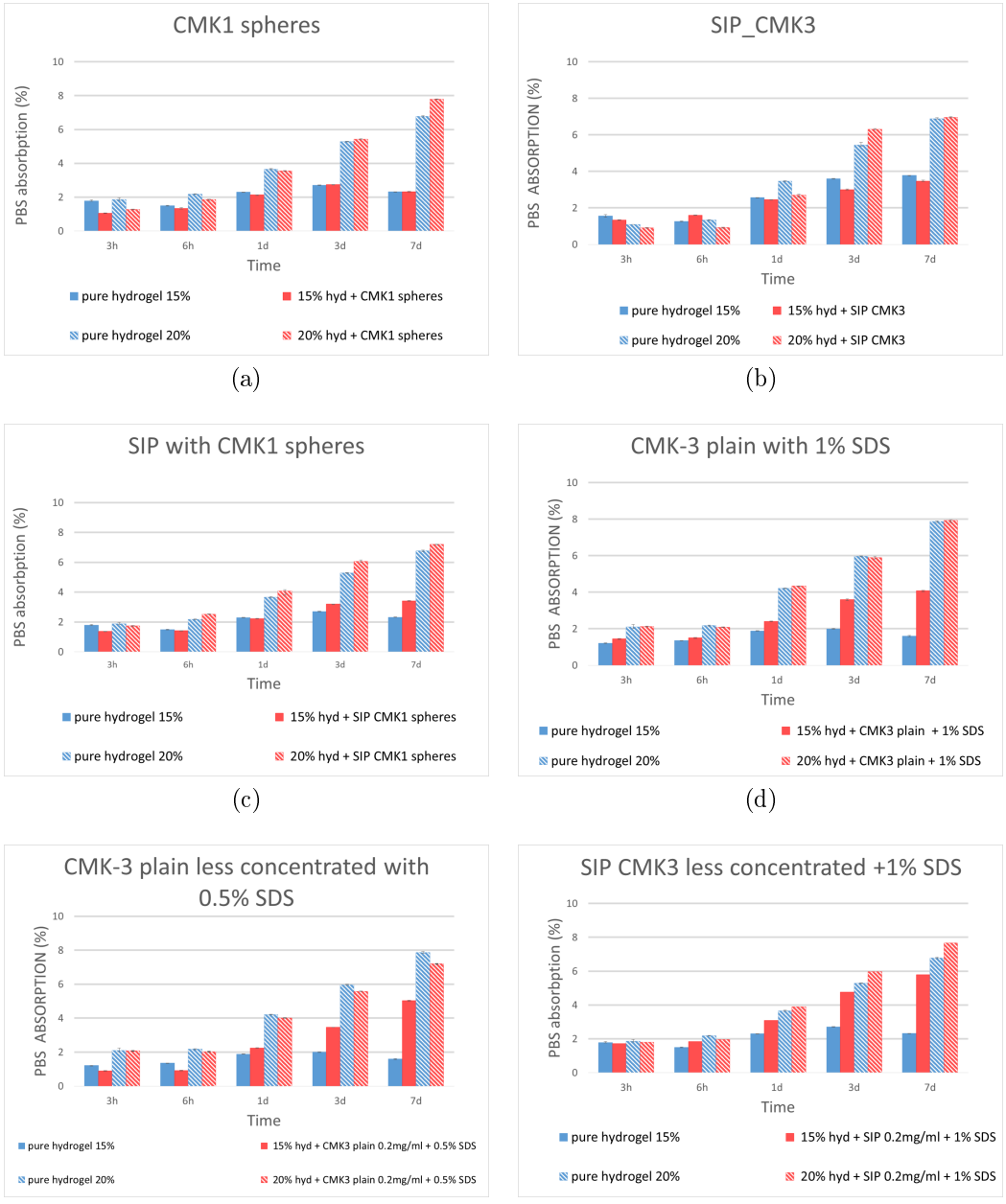

Figure 3.6: PBS absorption (%) in systems with (a) carbon shperical particles CMK1, (b) CMK3 coated with SIP, (c) carbon shperical particles CMK1 coated with SIP, (d) CMK3 plain irregular particles with 1% w/V of SDS with 2mg/ml concentration. The lats two graphs reported 0.2mg/ml of plain CMK3 with 0.5% w/V of SDS (e) and 0.2mg/ml of SIP coated CMK3 with 1% w/V of SDS (f).

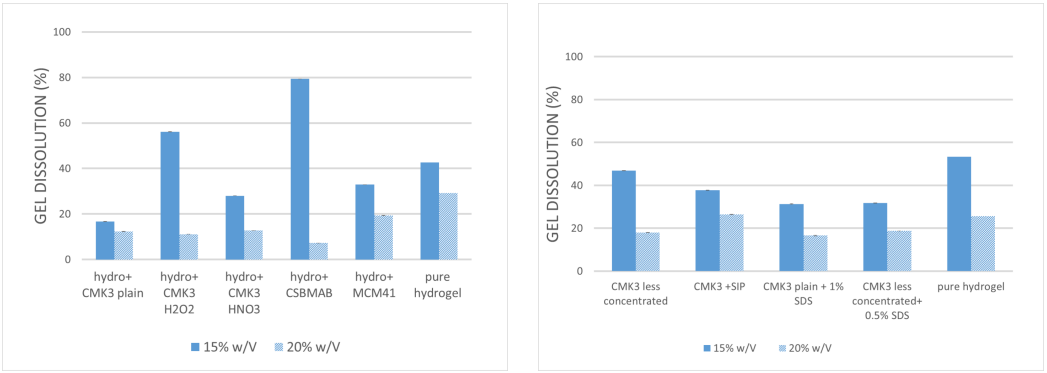

(a) (b)

Figure 3.7: Gel dissolution (%) for the composite systems with the particles compared with the pure hydrogel.

3.3 Morphology of the composite systems

After the tests performed to see if the hydrogel was affected by the presence of the particles, its surface and particles dispersion was evaluated through SEM analysis (Figure 3.8) on composite systems with MCM-41, CMK3 and CMK1 (details of synthesis and preparation in section 2.2.2).

Figure 3.8 proves that the particles are effectively present not only on the hydrogel surface, but also inside the pores. Silica particles seem to have the best dispersion, due to their hydrophilicity. Among the carbon particles, CMK1 seems to have the better dispersion than CMK3, probably due to their spherical shape against the typical rod-like shape of CMK3.

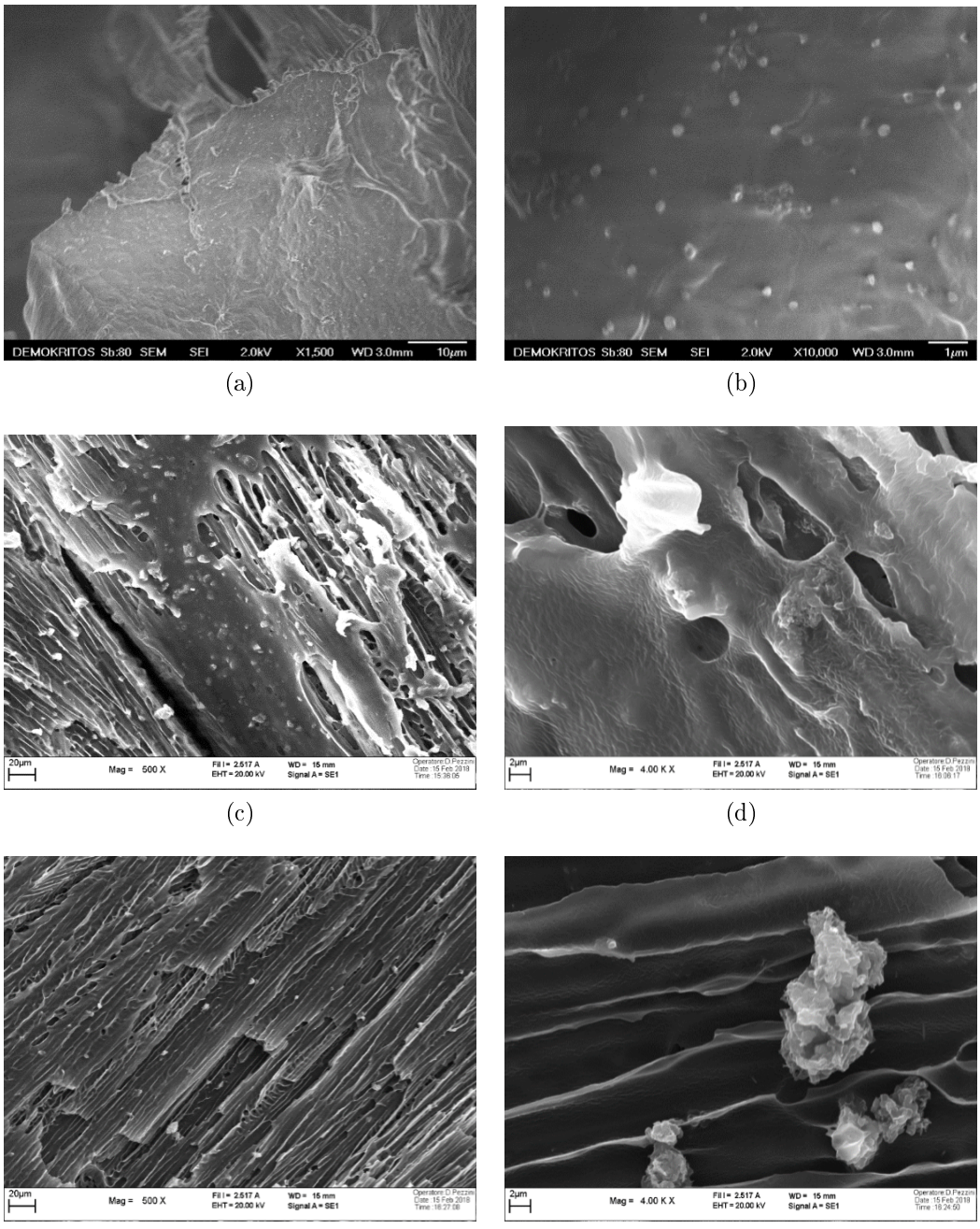

(a) (b)

(c) (d)

(e) (f)

Figure 3.8: SEM images of freeze dried sample of MCM-41 (a-b), CMK1(c-d) and CMK3 (e-f) with a 15% w/V hydrogel.

3.4 Drug loaded nanoparticles

The successful encapsulation of ibuprofen within the pores of nanoparticles was studied by TGA analysis on the IBU loaded particles and on a neat IBU sample. First of all, NPs and drug powders were mixed with a 1:1 ratio, and TGA analysis showed that this 1:1 ratio was maintained even after encapsulation. Indeed, Figure 3.9 shows that around 300 °C the drug evaporates. When this happens, the total mass of the composite systems decreases by approximately 50% of the initial weight, confirming the 1:1 initial loading.

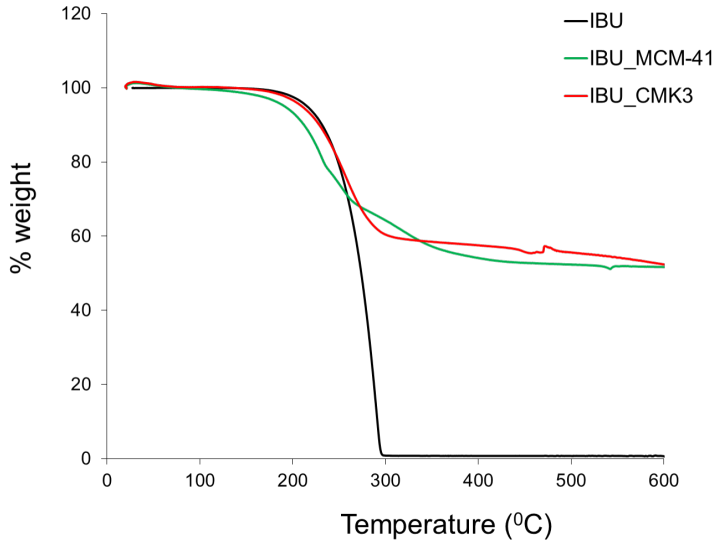

Figure 3.9: TGA analysis that shows weight variation (%) against temperature.

TGA analysis also proved that the drug was actually inside NPs pores, and not on the surface. As shown in Figure 3.10 the drug melts around 85 °C: this is melting point of the crystallized IBU. This peak is completely absent from the thermograms of the drug loaded carbon NPs indicating the absence of crystalline drug. Given that IBU has been proven to be in an amorphous and not crystalline form when confined in pores, this result provides evidence of the successful infiltration of the drug in the carbon NPs pores. The MCM-41 based sample shows a very small peak at this region suggesting that in this case a very small amount of drug may be left outside the pores. However this amount can be considered practically negligible when comparing the area of the peak with that of pure IBU.

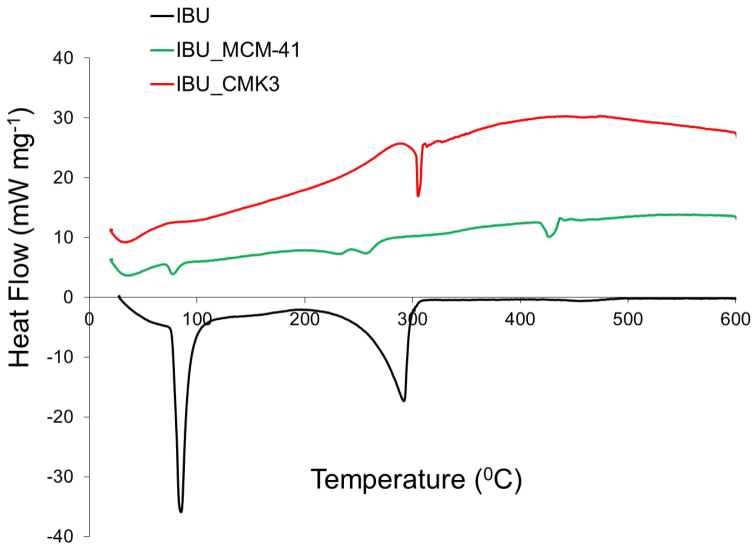

Figure 3.10: TGA analysis results - heat flow variations ($mWmg^{-1}$) against temperature.

3.5 Drug release results

The release of a drug from a hydrogel matrix involves different diffusion processes, inside and outside the system[50]. Exterior diffusion occurs when drug molecules diffuse from the surface of the matrix (where drug concentration is maximum) to the bulk of the release medium. When the bulk of the liquid is well stirred the value of drug concentration is constant. However, exterior diffusion does not usually control the rate of drug release, which in most cases depends on interior diffusion. Within the hydrogel matrix the drug is equally dissolved or dispersed in the polymer. For a one-dimensional slab-shaped system, unsteady-state drug diffusion can be described by Fick's second law of diffusion:

$$\frac{dC_A}{dx} = D\frac{d^2C_A}{dx^2} \tag{3.1}$$

where D, the drug diffusion coefficient, is assumed to be constant. For monolithic devices the system geometry (thin film, sphere, cylinder, irregular solid) affects strongly the resulting drug release profile. In the case of a device with initial drug concentration below drug solubility, the drug molecules are dissolved in the hydrogel (monolithic solution), otherwise the drug molecules coexist with amorphous aggregates and/or drug crystals (monolithic dispersion). For a monolithic solution, using the following release conditions:

1. the absence of significant changes in the hydrogel matrix during the release,
2. perfect sink conditions (the release medium is sufficiently dilute in a way not to impede desorption) during the release,
3. the release of drug is mostly controlled by diffusion through the hydrogel matrix,

different equations are used (as solutions of Eq. 3.1), to calculate a resulting release profile depending on the system geometry. For example:

- a membrane with uniform initial concentration of the diffusing substance and with negligible edge effects, the fractional release M_t/M_0 can be described by:

$$\frac{M_t}{M_0} = 1 - \frac{8}{\Pi^2}\sum_{n=0}^{\infty}\frac{1}{(2n+1)^2}\exp\left(\frac{-D(2n+1)^2\Pi^2 t}{L^2}\right) \tag{3.2}$$

  where: n - dummy variable, L - thickness of the film.

- for a spherical delivery device:

$$\frac{M_t}{M_0} = 1 - \frac{6}{\Pi^2} \sum_{n=0}^{\infty} \frac{1}{n^2} \exp\left(\frac{-Dn^2\Pi^2 t}{R^2}\right) \tag{3.3}$$

where: R - sphere radius.

- for a cylindrical delivery device:

$$\frac{M_t}{M_0} = 1 - \frac{32}{\Pi^2} \sum_{n=0}^{\infty} \frac{1}{q_n^2} \exp\left(\frac{-q_n^2 Dt}{R^2}\right) \cdot \cdot \sum_{p=0}^{\infty} \frac{1}{(2p+1)^2} \exp\left(\frac{-D(2p+1)^2\Pi^2 t}{H^2}\right) \tag{3.4}$$

where: p - dummy variable, q_n - roots of the Bessel function of the first kind of zero order, R - cylinder radius, H - cylinder height.

Assuming uniform initial distribution of the solute and that the surfaces of the system are kept at a constant concentration, a simplified, yet effective approximation for the determination of the diffusion coefficient D from measured desorption curves on a membrane is described by the following formula:

$$\theta = -\ln x + \frac{q}{p} + \frac{rq^2}{2p^3} \tag{3.5}$$

which is a solution of the Eq. 3.2, and where:

$\theta = \Pi^2 Dt/4l^2$
$x = \frac{1}{8}\Pi^2 M_t/M_\infty$
$p = 1 + x^8 + x^{24}$
$q = \frac{1}{9}x^8 + \frac{1}{25}x^{24}$
$r = 1 + 9x^8 + 25x^{24}$

The solution 3.5 is correct to four significant figures when $M_t/M_0 < 2/3$ for desorption from e.g. a plane sheet, or diffusion along a cylindrical rod or tube of length l, with one end and its surface sealed and the other end maintained at a constant concentration[51].

In the present work drug release tests were carried out on different systems in order to study the influence of different parameters on the process. Detailed description of samples preparation is reported in Section 2.3.

The gel systems directly loaded with ibuprofen did not exhibit distinct differences in terms of their drug release behavior. Indeed the fractional release vs time curves are quite similar, while all systems show initially a very rapid release, which evolves with a decreasing rate (Figure 3.11b). From Figure 3.11a it is clear how the samples loaded with more drug have a greater release. The volume of the gels was monitored throughout the release studies. Figure 3.12 shows how the IBU loading method involving ethanol caused a slow decrease of the gels' volume and ultimately their premature dissolution (this phenomenon is more pronounced for the system in which a larger amount of ethanol was used). The samples prepared without the organic solvent, on the contrary, showed some swelling. Both dissolution and swelling have a direct effect on the release behavior of the gel systems, which cannot be easily quantified (or controlled). As such diffusion coefficients were calculated based on Equation 3.5, mainly for the first 5-7 days of the release process, as it was observed that during this period the volume of all studied gels did not change significantly as shown in Figure 3.12. The deduced drug diffusion coefficient (D) values were found between $3.31 - 3.88 \cdot 10^{-11}\, m^2/s$.

The encapsulation of drug loaded NPs in the gels was seen to affect the kinetics of the release process. Figure 3.13 shows the fractional release curves from the composite gels with a relatively low amount of NPs (carrying 1 and 2 mg of ibuprofen). The types of nanoparticles and the variable loading did not seem to play a critical role in this case.

The comparison however of the release curves of the composites with those of the neat gels with similar initial loading points to slower release when the drug is carried through the NPs (Figure 3.14). The respective diffusion coefficients were found within the range $2.11 - 2.83 \cdot 10^{-11} m^2/s$.

The slower and thus more controlled release is even more evident for the composite systems loaded with 20 mg of NPs (10 mg of IBU), as shown in Figure 3.15 which however showed a premature decrease of their volume accompanied by the depletion of the NPs. Nevertheless the respective diffusion coefficients were one order of magnitude lower, within the range $3.85 - 3.98 \cdot 10^{-12}\, m^2/s$.

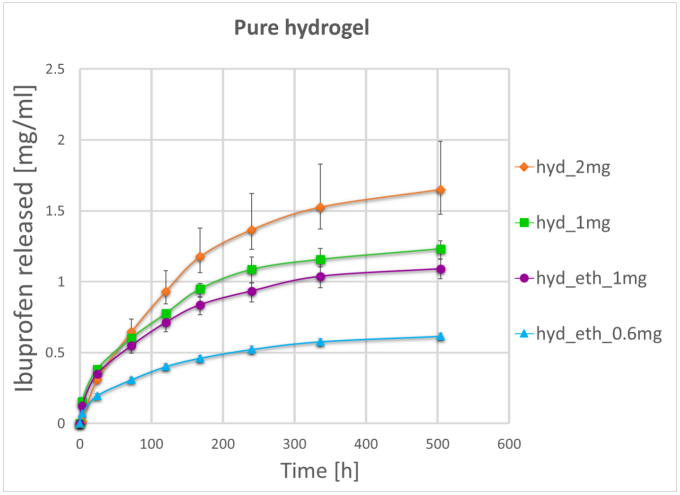

(a)

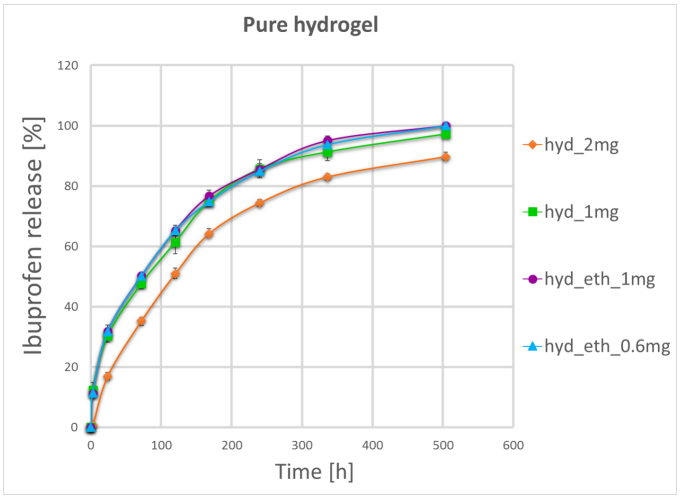

(b)

Figure 3.11: Pure hydrogel release curves: samples loaded with 2 mg and 1 mg of IBU simply mixing the powders (orange and green, respectively), samples loaded with 1 mg and 0.6 mg of IBU pre-dispersing it in ethanol (purple and blue, respectively).

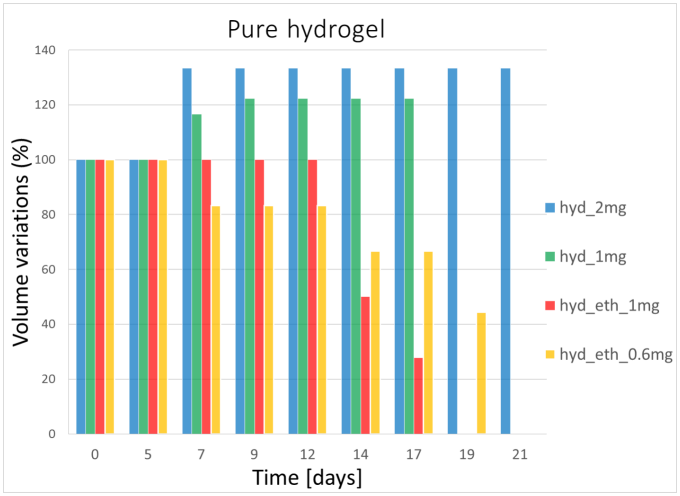

Figure 3.12: Volume variations (%) of pure hydrogel samples.

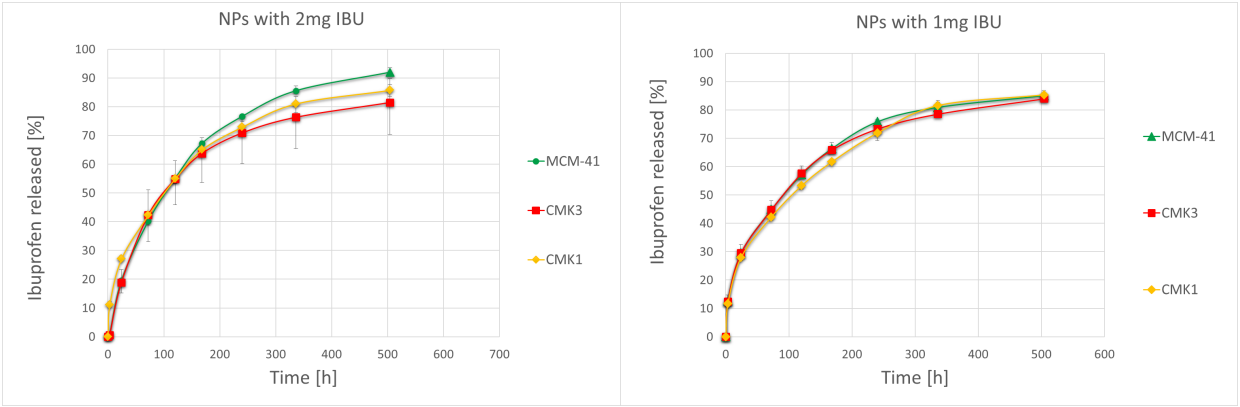

(a) (b)

Figure 3.13: Nanocomposite systems release curves: samples loaded with a) 2 mg and b) 1 mg of IBU.

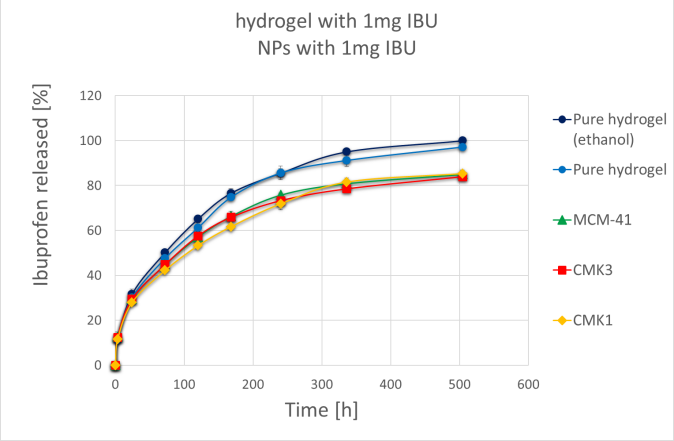

Figure 3.14: Release curves of samples loaded with 1 mg of IBU of pure hydrogel prepared pre-dispersing the drug in ethanol (dark blue) and pure hydrogel prepared simply mixing the drug (light blue) and composite systems - MCM-41 (green), CMK3 (red), CMK1 (yellow).

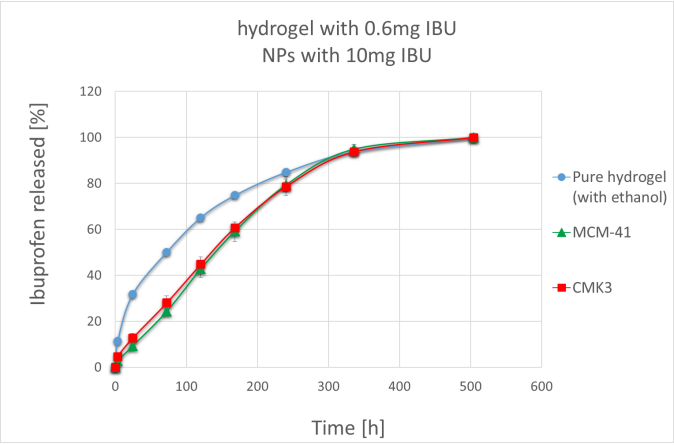

Figure 3.15: Release curves of pure hydrogel samples loaded with 0.6 mg of IBU prepared pre-dispersing the drug in ethanol (blue) and composite systems loaded with 10mg of IBU- MCM-41 (green), CMK3 (red), CMK1 (yellow).

4 CONCLUSIONS

The present work is the result of a collaborative work between Politecnico di Torino and the INRASTES/INN institutes of the National Center for Scientific Research Demokritos (Athens, Greece).

The goal was to realize composite systems based on hydrogel and ordered mesoporous materials (carbon and silica) to obtain a controlled drug release. The drug used during the work was the nonsteroidal anti-inflammatory ibuprofen (IBU).

First of all, silica nanoparticles were successfully synthesized. Carbon particles and hydrogel were used ready, previously prepared at the NCSR "Demokritos" laboratory and at Politecnico di Torino, respectively. NPS characterization was performed using SEM, FTIR, N_2 porosimetry, PXRD. They showed to have a good morphology (spherical for MCM-41 and CMK1 and rods for CMK3) with uniform size, N_2 adsorption-desorption curves characteric of mesoporous materials, great surface area ($\sim 1000 - 2000\, m^2/g$) and great pore volume ($\sim 1.0 - 1.8\, cm^3/g$).

Then, both silica and carbon particles were incorporated into the hydrogel testing different protocols, aiming at the same time to have a good dispersion and to maximize particles content. Silica particles did not show any particular difficulties in their handling, due to their hydrophilic nature. On the other hand, carbon particles required a greater effort, since they are hydrophobic. Thus, a large amount of different particles has been tested to achieve the purpose -irregular and spherical particles, functionalized particles following various routes, to have functional groups on the surface that helps the dispersion. In addiction, the use of SDS surfactant and the SIP coating was also tested.

After all these trials, a very good dispersion has been achieved, showing that a concentration of 1% w/V of the SDS surfactant helps to disperse carbon particles in a very large extent, and the hydrogel is not affected by its presence.

The composite systems with the particles were evaluated in terms of gelation time, tube inverting test, stability and dissolution test. Furthermore, sample surface and dispersion was evaluated with SEM images. These tests show that the hydrogel is not affected -neither in terms of structure nor behaviour- by the presence of the nanoparticles. Thus, the composite material showed to be a very good candidate for the drug release tests, also carried out on the pure hydrogel -as reference.

Initially, the drug was loaded into the particles using a melt infiltration procedure

that allows it to get encapsulated into the NPs pores. TGA analysis showed that the drug was loaded successfully.

IBU loading into the pure hydrogel is not straightforward due to its hydrophobic nature. Therefore, it was carried out in two ways, either pre-dispersing it in an ethanol solution and simply mixing it with gel grains, helping the dispersion using SDS. This is a limit, because it sets a an upper limit on the maximum amount of loadable drug. In the first case the problem is the organic solvent, because it affects the hydrogel. While in the latter, the problem is the incomplete IBU dissolution. Hence, the presence of the particles represents a great improvement, because drug could been successfully loaded with a 1:1 ratio with particles. Indeed, 10mg of IBU was loaded in the composite systems. Furthermore, the presence of ethanol showed to be very negative for the hydrogel, since the samples whose preparation involved its use, had a great decrease in the volume until a complete premature dissolution.

Drug release in the composite material showed to be slower than in the pure hydrogel, verifying that the encapsulation of drug loaded nanoparticles in the hydrogel matrix can indeed lead to a more controlled and prolonged release of a larger amount of the active compound. This was also proved trough the determination of the diffusion coefficients D of pure hydrogel samples and of composite samples with a simplified but effective approximation. In the latter case, D coefficient was lower, confirming a slower release.

Acknowledgements

I would like to thank professor Gianluca Ciardelli for his helpfulness, for following me, though not from close distance, with commitment and attention.

I would like to thank with all my heart my supervisor in Greece, dr. Georgia Charalamboupoulou. First of all, this work was possible thanks to your guide and your contribution, you guided me with patience and care. But beyond that, I wanted to thank you for always being a referring point for me during my period in Athens. You have done more than what was your duty. Thank you very much!

A great thanks to Dimitra, Lamprini, Vana...For your huge contribution in my work, and for always being ready to help me, in the lab and outside the lab. But mostly, thank you for making the work environment always cheerful and friendly!! And thank you to all the people from Demokritos, all of you are wonderful people. I wish you all the best!

A special thanks even to dr. Monica Boffito and to dr. Chiara Tondaturo. You have always followed me with great attention and precision during all the writing period. Thank you for always being so helpful, but also so kind!

Thanks to my parents, to which I dedicate my successes, because without them I would have never been where I am. You are always my strength! And to my brother, for your scientific cooperation, but also for your love.

To Giuseppe, you've always been there for me, even if we weren't so close.

Ringraziamenti

Vorrei ringraziare il prof. Gianluca Ciardelli per la sua disponibilità, per avermi seguito, seppur a distanza, con impegno e attenzione.

Un grazie di cuore alla mia relatrice in Grecia, la dott.ssa Georgia Charalamboupoulou. Prima di tutto, perché questo lavoro è stato possibile grazie alla tua guida e al tuo contributo, mi hai guidato con pazienza e attenzione. Ma oltre questo, volevo ringraziarti per essere sempre stata un punto di riferimento per me durante il mio periodo ad Atene. Hai fatto molto di più di quello dovevi. Grazie mille!

Un grandissimo grazie anche a Dimitra, Lamprini, Vana...Per l'enorme contributo in questo lavoro, e per essere sempre state pronte ad aiutarmi, in laboratorio e fuori. Ma soprattutto, grazie per aver reso l'ambiente sempre allegro e amichevole. E grazie a tutti quanti i colleghi di Demokritos, delle persone meravigliose.

Un ringraziamento speciale anche alla dott.ssa Monica Boffito e alla dott.ssa Chiara Tondaturo, per avermi sempre seguito con grande attenzione e precisione durante tutto il periodo di stesura. Grazie per essere sempre state così disponibili, ma anche sempre gentili!

Grazie ai miei genitori, a cui dedico i miei successi, perché senza di loro non sarei mai arrivata dove sono. Siete la mia forza, sempre! E grazie a mio fratello, per il tuo contributo scientifico e affettivo.

A Giuseppe, che ci sei sempre stato, anche se lontano.

Bibliography

1. G. Tiwari, R. Tiwari , B. Sriwastawa, L. Bhati, S Pandey, P Pandey, and S Bannerjee, Drug delivery systems: An updated review, Int J Pharm Investig. 2012 Jan-Mar; 2(1): 2–11.

2. Nevozhay D, Kañska U, Budzyñska R, Boratyñski J, Current status of research on conjugates and related drug delivery systems in the treatment of cancer and other diseases (Polish). Postepy Hig Med Dosw, 2007, 61, 350–360

3. M. Boffito, E. Gioffredi, V Chiono, S Calzone, E Ranzato, S Martinotti and G Ciardelli, Novel polyurethane-based thermosensitive hydrogels as drug release and tissue engineering platforms: design and in vitro characterization, Polym Int, 2016; 65: 756–769

4. J. Kopeček, Hydrogel Biomaterials: A Smart Future?, Biomaterials, 2007 Dec; 28(34): 5185–5192.

5. B. B. Subudhi, S. Mandal, Self-Microemulsifying Drug Delivery System: Formulation and Study Intestinal Permeability of Ibuprofen in Rats, Hindawi Publishing Corporation, Journal of Pharmaceutics, Volume 2013, Article ID 328769, http://dx.doi.org/10.1155/2013/328769

6. Steve I. Shen, Bhaskara R. Jasti, and Xiaoling Li, Standard Handbook of Biomedical Engineering and Design, Chapter 22: Design of controlled-release drug delivery systems, The McGraw-Hill Companies, Inc. 2003

7. D. J. Greenblatt, M.D., Elimination half-life of drugs: value and limitations, Ann. Rev. Med. 1985. 36: 421-27

8. I. Khan, K. Saeed, I. Khan, Nanoparticles: Properties, applications and toxicities, Arabian Journal of Chemistry (2017), http://dx.doi.org/10.1016/j.arabjc.2017.05.011

9. Roy R, Roy RA, Roy DM. Alternative perspectives on "quasi-crystallinity": non-uniformity and nanocomposites. Materials Letters. 1986; 4(8-9):323-328.

10. P. H. C. Camargo; K. G. Satyanarayana; F. Wypych, Nanocomposites: synthesis, structure, properties and new application opportunities, Mat. Res. vol.12 no.1 São Carlos Jan./Mar. 2009

11. A. H. Faraji, P. Wipf, Nanoparticles in cellular drug delivery, Bioorganic & Medicinal Chemistry 17 (2009) 2950–2962

12. W. H. De Jong, P. J. Borm, Drug delivery and nanoparticles: applications and hazards, International Journal of Nanomedicine, 2008, 133-149

13. Kiamahalleh MV, Mellati A, Madani SA, Pendleton P, Zhang H, Madani SH, Smart carriers for controlled drug delivery: thermosensitive polymers embedded in ordered mesoporous carbon, Journal of Pharmaceutical Sciences (2017), doi: 10.1016/j.xphs.2017.02.010.

14. R. Xu, G. Zhang, J. Mai, X. Deng, V. Segura-Ibarra, S. Wu, J. Shen, H. Liu, Z. Hu, L. Chen, Y. Huang, E. Koay, Y. Huang, J. Liu, J. E. Ensor, E. Blanco, X. Liu, M. Ferrari, H. Shen, An injectable nanoparticle generator enhances delivery of cancer therapeutics, Nature Biotechnology volume 34, pages 414–418 (2016)

15. S. K. H. Gulrez, S. Al-Assaf and G. O. Phillips, Hydrogels: Methods of Preparation, Characterisation and Applications, 2011

16. E. Caló, V.V. Khutoryanskiy, Biomedical applications of hydrogels: A review of patents and commercial products, European Polymer Journal 65 (2015) 252–267

17. M. Boffito, P. Sirianni, A. M. Di Rienzo, V. Chiono, Thermosensitive block copolymer hydrogels based on poly(E-caprolactone) and polyethylene glycol for biomedical applications: State of the art and future perspectives, journal of biomedical materials research, mar 2015 vol 103a, issue 3

18. M. Gisbert-Garzarán, M. Manzano and M. Vallet-Reg, pH-Responsive Mesoporous Silica and Carbon Nanoparticles for Drug Delivery, Bioengineering 2017, 4(1), 3; doi:10.3390/bioengineering4010003

19. Gisbert-Garzaran, M., Lozano, D., Vallet-Regí, M., Manzano, M., Self-immolative polymers as novel pH-responsive gate keepers for drug delivery. RSC Adv., 2017, 7(1), 132 – 136

20. W. Li and D. Zhao, "An overview of the synthesis of ordered mesoporous materials, Chem. Commun., 2013

21. L. Mahoney and R. Koodali, Versatility of Evaporation-Induced Self-Assembly (EISA) Method for Preparation of Mesoporous TiO2 for Energy and Environmental Applications, Materials 2014, 7, 2697-2746; doi:10.3390/ma7042697

22. F. Raji, M. Pakizeh, Study of Hg(II) species removal from aqueous solution using hybrid $ZnCl_2-MCM-41$ adsorbent, Applied Surface Science 282 (2013) 415–424

23. A. I., Ojumu T. V., Ogunfowokan A. O., Biomass, Abundant Resources for Synthesis of Mesoporous Silica Material, 2016, Microporous and Mesoporous Materials, http://dx.doi.org/10.5772/63463,

24. Bharti C, Nagaich U, Pal AK, Gulati N. Mesoporous silica nanoparticles in target drug delivery system: A review. International Journal of Pharmaceutical Investigation. 2015;5(3):124-133. doi:10.4103/2230-973X.160844.

25. D. Zhao, Q. Huo, J. Feng, B.F. Chmelka, G.D. Stucky, J. Am. Chem. Soc. 120 (1998) 6024–6036

26. S.M.L. dos Santos, K. Nogueira, M. de Souza Gama, J. Ferreira Lima, I. da Silva Júnior, D. de Azevedo, Synthesis and characterization of ordered mesoporous silica (SBA-15 and SBA-16) for adsorption of biomolecules, Microporous and Mesoporous Materials 180 (2013) 284–292

27. P. F. Fulvio a , S. Pikus, M. Jaroniec, Short-time synthesis of SBA-15 using various silica sources, Journal of Colloid and Interface Science 287 (2005) 717–720

28. R. Ryoo, S. H. Joo, M. Kruk, M. Jaroniec, Ordered Mesoporous Carbons, Advanced Materials, 2001, 13, No. 9, May 3

29. W. Xin and Y. Song, Mesoporous carbons: recent advances in synthesis and typical applications, RSC Adv., 2013, DOI: 10.1039/C5RA16864C

30. D. Giasafaki, A. Bourlinos, G. Charalambopoulou, A. Stubos, T. Steriotis, Nanoporous carbon - metal composites for hydrogen storage, Cent. Eur. J. Chem., 9(5), 2011, 948-952, DOI: 10.2478/s11532-011-0081-z

31. P. Niebrzydowska, R. Janus, P. Kustrowski, S. Jarczewski, A. Wach, A. M. Silvestre-Albero, F. Rodrıguez-Reinoso, A simplified route to the synthesis of CMK-3 replica based on precipitation polycondensation of furfuryl alcohol in SBA-15 pore system, Carbon, 64 (2013) 252–261

32. R. Ryoo, S. H. Joo, and S. Jun, Synthesis of Highly Ordered Carbon Molecular Sieves via Template-Mediated Structural Transformation, J. Phys. Chem. B, Vol. 103, No. 37, 1999

33. Jun S, Joo SH, Ryoo R, Kruk M, Jaroniec M, Liu Z, Ohsuna, O. Terasaki, Synthesis of new, nanoporous carbon with hexagonally ordered mesostructure, J Am Chem Soc 2000;122:10712–3.

34. A. Eftekhari and Z. Fan, Ordered mesoporous carbon and its applications for electrochemical energy storage and conversion, Mater. Chem. Front., 2017, 1, 1001—1027

35. Matthias Thommes, Katsumi Kaneko, Alexander V. Neimark, James P. Olivier, Francisco Rodriguez-Reinoso, Jean Rouquerol, Kenneth S.W. Sing, Physisorption of gases, with special reference to the evaluation of surface area and pore size distribution (IUPAC Technical Report), Pure Appl. Chem. 2015

36. Stuart B., Infrared Spectroscopy: Fundamentals and Applications, John Wiley & Sons,2004

37. J. M. Loureiro, M. T. Kartel, Combined and Hybrid Adsorbents - Fundamentals and Applications, Published by Springer,2005

38. J. C. Su, S. Q. Liu, Sunil C. Joshi and Y. C. Lam, Effect of SDS on the gelation of hydroxypropylmethylcellulose hydrogels, Journal of Thermal Analysis and Calorimetry, Vol. 93 (2008) 2, 495–501

39. Shin YM, Kwon TH, Kim KS, Chae KS, Kim DH, Kim JH, Yang MS. Enhanced iron uptake of Saccharomyces cerevisiae by heterologous expression of a tadpole ferritin gene. Appl Environ Microbiol 67(3):1280-3 (2001)

40. Lu, A.-H., Li, W.-C., Schmidt, W., Schu¨th, F., Template synthesis of large pore ordered mesoporous carbon. Microporous Mesoporous Mater. 80, 117–128 (2005)

41. http://hyperphysics.phy-astr.gsu.edu/hbase/index.html

42. https://chem.libretexts.org/

43. Monty Liong, Jie Lu, Michael Kovochich, Tian Xia, Stefan G. Ruehm, Andre E.Nel, Fuyuhiko Tamanoi,Jeffrey I. Zink, Multifunctional Inorganic Nanoparticles for Imaging, Targeting, and Drug Delivery, ACS Nano. 2008 May ; 2(5): 889–896. doi:10.1021/nn800072t.

44. C. P. Reis, J. P. Ferreira, S. Candeias, C. Fernandes, N. Martinho, N. Aniceto, A. S. Cabrita, I. V. Figueiredo, Ibuprofen Nanoparticles for Oral Delivery: Proof of Concept, J Nanomedine Biotherapeutic Discov 2013, http://dx.doi.org/10.4172/2155-983X.1000119

45. U. Gulyuz , O. Okay, Self-Healing Poly(acrylic acid) Hydrogels:Effect of Surfactant, Macromol. Symp. 2015, 358, 232–238

46. Wang, J., Liu, Q. Nitrogen loss and structural change of nitrogen-incorporated SBA-15 mesoporous materials under different treatment conditions. J. Mater. Res.20, 2296–2301 (2005).

47. Wang, J., Liu, Q. F., Liu, Q. Synthesis and characterization of Sn or Al-containing SBA-15 mesoporous materials without mineral acids added. Microporous Mesoporous Mater. 102, 51–57 (2007).

48. Kaneda, M. et al. Structural study of mesoporous MCM-48 and carbon networks synthesized in the spaces of MCM-48 by electron crystallography. J. Phys. Chem. B106, 1256–1266 (2002).

49. R.A. Petros, J.M. DeSimone, Strategies in the design of nanoparticles for therapeutic applications, Nat Rev Drug Discov, 9 (2010) 615-27

50. R. Zarzycki, Z. Modrzejewska, K. Nawrotek, Drug Release form Hydrogel Matrices, Ecological Chemistry and Engineering. S, 17(2) 2010, 117-139

51. J. Crank, The Mathematics of Diffusion, 2nd Edition, Clarendon Press, Oxford, UK, 1975, Chapter 4